ESTCP
Cost and Performance Report

(MM-0741)

Next Generation HeliMag UXO Mapping Technology

January 2010

ENVIRONMENTAL SECURITY
TECHNOLOGY CERTIFICATION PROGRAM

U.S. Department of Defense

COST & PERFORMANCE REPORT
Project: MM-0741

TABLE OF CONTENTS

Page

1.0 EXECUTIVE SUMMARY 1

2.0 INTRODUCTION 3
- 2.1 BACKGROUND 3
- 2.2 OBJECTIVES OF THIS DEMONSTRATION 3
- 2.3 REGULATORY DRIVERS 4

3.0 TECHNOLOGY 5
- 3.1 TECHNOLOGY DESCRIPTION 5
  - 3.1.1 Helicopter Platform 6
  - 3.1.2 Sensors and Sensor Configuration 6
  - 3.1.3 Positioning Technologies 6
  - 3.1.4 Telemetry System 6
  - 3.1.5 Data Acquisition System 6
  - 3.1.6 Data Processing 7
  - 3.1.7 Data Analysis 7
- 3.2 TECHNOLOGY DEVELOPMENT 7
  - 3.2.1 System Component Development and Updates 7
  - 3.2.2 Sensors and Sensor Configuration 8
  - 3.2.3 Noise Suppression Algorithm 8
  - 3.2.4 Telemetry System 9
  - 3.2.5 Shakedown Tests 9
- 3.3 ADVANTAGES AND LIMITATIONS OF THE TECHNOLOGY 9

4.0 PERFORMANCE OBJECTIVES 11

5.0 SITE DESCRIPTION 13
- 5.1 SITE LOCATION AND HISTORY 13
- 5.2 SITE GEOLOGY 13
- 5.3 MUNITIONS CONTAMINATION 13

6.0 TEST DESIGN 15
- 6.1 CONCEPTUAL EXPERIMENTAL DESIGN 15
- 6.2 SITE PREPARATION 16
- 6.3 SYSTEM SPECIFICATION 16
- 6.4 DATA COLLECTION 16
- 6.5 VALIDATION 18

7.0 DATA ANALYSIS AND PRODUCTS 19
- 7.1 PREPROCESSING 19

TABLE OF CONTENTS (continued)

Page

7.2 TARGET SELECTION FOR DETECTION 19
7.3 PARAMETER ESTIMATES 19
7.4 CLASSIFIER AND TRAINING 19
7.5 DATA PRODUCTS 20
7.5.1 Raw Data 20
7.5.2 Target Lists 20

8.0 PERFORMANCE ASSESSMENT 23
8.1 EASE OF USE 25
8.2 GEOREFERENCE POSITION ACCURACY 25
8.3 DETECTION PERFORMANCE 26
8.3.1 Scenario 1: Ground Vehicle, 2005 AMTADS and 2009 HeliMag Data 26
8.3.2 Scenario 2: 2005 AMTADS and 2009 HeliMag Data 26
8.3.3 Scenario 3: Detection of Blind Seeded Targets 26
8.3.3.1 60 and 81 mm Mortars in the North-Central Seed Area 26
8.3.3.2 Detection Results in the Geologically Challenging Western Seed Area 30
8.4 TELEMETRY LINK 30
8.5 NOISE LEVEL 32
8.6 ACCURACY OF CALCULATED VERTICAL GRADIENTS 33
8.7 UXO PARAMETER ESTIMATE REPEATIBILITY 33
8.8 OPERATING PARAMETERS 35
8.9 ROTOR NOISE SUPPRESSION ALGORITHM 35
8.10 DATA DENSITY/POINT SPACING 37
8.11 SURVEY COVERAGE 37

9.0 COST ASSESSMENT 39
9.1 DATA PROCESSING AND ANALYSIS, REPORTING 40
9.2 MANAGEMENT 41
9.3 COST DRIVERS 41
9.4 COST BENEFIT 41

10.0 IMPLEMENTATION ISSUES 43

11.0 REFERENCES 45

APPENDIX A POINTS OF CONTACT A-1

LIST OF FIGURES

Page

Figure 1. SKY next generation HeliMag system. 5
Figure 2. Former Kirtland Precision Bombing Range with HeliMag 2009 test areas superimposed on HeliMag data collected in 2005 14
Figure 3. Overview of survey data collected. 17
Figure 4. Estimated locations of items on the validation lane for all 4 days with the lane flown twice per day. 25
Figure 5. Seeded target SNRs for the HeliMag system and simulated AMTADS system 28
Figure 6. Pseudo ROC curves for seeded targets, and graphs of total detections and Pd plotted as a function of SNR cutoff threshold for the HeliMag data and simulated AMTADS data 29
Figure 7. Comparison of target classification distribution between all 983 targets in the seeded area and the 49 detected seeds 29
Figure 8. Comparison between measured and calculated gradients over the validation line flown on the last flight of day 78. 33
Figure 9. Dipole parameters estimated from the validation lane data. 34
Figure 10. Data from the middle sensor (sensor 7) collected at high-speed over the validation line on day 78. 36
Figure 11. Close-up of validation lane anomalies from Figure 10, showing the difference between the raw data, a 6 Hz low-pass filtered version of the data and the rotor-noise corrected data. 37

LIST OF TABLES

Page

Table 1. Sky research next generation HeliMag technology components. 5
Table 2. Performance objectives and results. 11
Table 3. Flight parameters for data collection. 16
Table 4. Performance objective results. 23
Table 5. Classes used in the interpretation of the seed area data. 26
Table 6. Scoring results as generated by IDA for the seed targets in the north-central area. 27
Table 7. Seed detection results in the western seed area. 31
Table 8. Number of seed items and detected items in each category for the western seed area. 32
Table 9. Standard deviations of the compensated (but not filtered) high-altitude data. 32
Table 10. Standard deviations of dipole fit parameters on the validation lane data. 34
Table 11. Survey altitude and speed for each area. 35
Table 12. Cost tracking. 39
Table 13. Projected costs for 2-day survey using the next generation HeliMag system. 40
Table 14. Estimated costs scenarios for helicopter magnetometry. 40

ACRONYMS AND ABBREVIATIONS

206L	Bell 206 Long Ranger
agl	above ground level
Am^2	ampere-meter(s) squared
AMTADS	Airborne Multisensor Towed Array Detection System
AS	analytic signal
ASR	Archive Search Report
C&P	Cost and Performance
CERCLA	Comprehensive Environmental, Response, Compensation, and Liability Act
CRADA	Cooperative Research and Development Agreement
Cs	cesium
CSM	conceptual site model
DAS	Data Acquisition System
dB	decibel(s)
DC	direct current
DEM	digital elevation model
DGM	digital geophysical mapping
DoD	Department of Defense
EM	electromagnetic
ESTCP	Environmental Security Technology Certification Program
FLBGR	Former Lowry Bombing and Gunnery Range
FUDS	Formerly Used Defense Sites
GPS	Global Positioning System
HE	high explosive
HEAT	high explosive anti-tank
HeliMag	helicopter magnetometry
HR	HEAT-round
ID	Identification
IDA	Institute for Defense Analyses
IMU	inertial measurement unit
IPR	Interim Progress Review
KPBR	Kirtland Precision Bombing Range
Kts/hr	knots per hour
LiDAR	Light Detection and Ranging

ACRONYMS AND ABBREVIATIONS (continued)

MD	McDonnell Douglas
µs	microsecond
MMRP	Military Munitions Response Program
MTADS	Multisensor Towed Array Detection System
m/s	meters per second
NDIA	New Demolitions Impact Area
NRL	Naval Research Laboratory
nT	nanotesla
OB/OD	open burn/open detonation
Pd	percentage of detection
Pfa	probability of false alarm
QC	Quality Control
ROC	receiver operating characteristic
RTK GPS	real-time kinematic global positioning system
SAIC	Science Applications International Corporation
SERDP	Strategic Environmental Research and Development Program
SKY	Sky Research, Inc.
SNR	signal-to-noise ratio
SORT	simulated oil refinery target
STC	supplemental type certification
TMF	total magnetic field
USACE	U.S. Army Corps of Engineers
USEPA	U.S. Environmental Protection Agency
UXO	unexploded ordnance
V	volt(s)
VNC	virtual network computing
VSEMS	Vehicular Simultaneous Electromagnetic Induction and Magnetometer System
WWII	World War II
WAA	wide area assessment

ACKNOWLEDGEMENTS

This Next Generation HeliMag Unexploded Ordnance (UXO) Mapping Technology Cost and Performance (C&P) Report documents the performance achieved during the technology demonstration, as well as the costs to conduct the demonstration and projected costs for future deployments. The testing was conducted at the Former Kirtland Precision Bombing Range near Albuquerque, NM. The work was performed by Sky Research, Inc. of Oregon, with Dr. Stephen Billings serving as principal investigator and Mr. David Wright of Wright Research and Design serving as co-principal investigator.

Funding for this project was provided by the Environmental Security Technology Certification Program (ESTCP) Office. This project offered the opportunity to examine advanced airborne methods as part of the Department of Defense's (DoD) efforts to evaluate wide area assessment technologies for the efficient characterization and investigation of large DoD sites.

We wish to express our sincere appreciation to Dr. Jeffrey Marqusee, Dr. Anne Andrews, Dr. Herb Nelson, and Ms. Katherine Kaye of the ESTCP Office for providing support and funding for this project.

Technical material contained in this report has been approved for public release.

This page left blank intentionally.

1.0 EXECUTIVE SUMMARY

A number of technical innovations were made to an existing helicopter magnetometry (HeliMag) platform to improve performance in wide area assessment applications. The HeliMag technology was originally developed by the Naval Research Laboratory (NRL), for deployment of seven total-field magnetometers on a Kevlar reinforced boom mounted on a Bell 206L helicopter. The objectives of this demonstration were to:

- Improve data acquisition speeds through implementation of advanced data sampling and noise suppression methodologies
- Enhance HeliMag detection by optimizing sensor configurations (to ensure that the magnetic field is fully and optimally sampled), and by improving noise suppression techniques (to maximize the signal-to-noise ratio [SNR] of targets of interest)
- Enhance HeliMag data interpretation using automated detection and characterization algorithms to improve productivity and produce objective, repeatable results
- Implement real-time data telemetry to remove the requirement to have a systems operator on board the aircraft, thereby increasing productivity, expanding applicability, and reducing risk.

A design study was conducted to select the telemetry components and decide on the deployment configuration. We determined that any operational advantage achieved by real-time telemetry of the actual sensor data was not significant enough to warrant the complexity of a telemetry system that would be required to allow that goal to be achieved. The ability to transmit information on the state of the system to the ground crew was determined to be a more realistic and mission-critical requirement. For this task, an omni-directional HD Communications Corp antenna was selected for mounting on the helicopter. An MP-Tech puck sector antenna, which needs to be manually pointed towards the helicopter during operation, was selected as the ground station antenna. A Tranzeo TR-600 radio, which meets both 802.11b and 802.11g communication standards, was selected for the broadcast and receive tasks. To monitor the data quality and allow remote interaction with the computer on the helicopter, we used virtual network computing (VNC) viewer software.

A sensor optimization study was conducted to determine if additional sensors were needed and, if so, where they should be placed for optimal detection and characterization performance. It was found that the optimal configuration was to decrease the sensor spacing from 1.5 m to 0.75 m, thus increasing the number of sensors from seven to 13. Full sampling of the magnetic field occurs whenever the sensors are greater than 1.5 m above the ground. Potential field theory can then be used to calculate the magnetic field at any higher elevation so that vertical gradients can be calculated rather than measured as in competing systems.

We mounted the modified sensor boom on a Hughes McDonnell Douglas (MD)530F helicopter. The dominant noise source in the system was found to originate from the rotor hub and resulted in a largely sinusoidal signal with a frequency of about 7.8 Hz. When flying low and fast, the

frequency band of the rotor noise overlaps with that of the signals of interest and the noise can't simply be eliminated by a notch filter. A new technique for rotor noise suppression was developed as part of this project. It uses data collected during a high-altitude aeromagnetic compensation flight to provide a model of the amplitude of the rotor-noise as a function of helicopter attitude. The phase of the rotor-noise varies as a function of helicopter attitude and is calculated along short segments. The algorithm can successfully suppress the rotor noise without distorting the spatial signature of the underlying anomalies of interest.

A demonstration study was conducted over 586 acres at the Former Kirtland Precision Bombing Range (KPBR) in New Mexico. The area covered overlapped a previous survey with the original system along with a number of ground-based surveys. Two areas were blind seeded with a number of ordnance with calibers ranging from 60 to 155 mm.

Three different locations were used as base stations for the telemetry. During the demonstration the telemetry system worked extremely well, with connectivity maintained for between 70 to 100 percent (%) of the time during each survey event. On average, connectivity was maintained for greater than 95% of the time. With this type of performance, removing the sensor operator from the helicopter is a viable option, with associated reduction in the risk and cost of the technology.

Detection performance was evaluated on two seeded sites. The first in the central north area consisted of 40 60 mm mortars and 40 81 mm mortars. With a halo of 1 m, 23% of the 60 mm mortars and 100% of the 81 mm mortars were detected. The poor detection performance on the 60 mm mortars occurred because the sensor ground clearance was too high (~1.8 m) compared to our intended ground clearance (1.0 m). Previous operational experience with the precursor system had revealed considerable variability in the flying heights achieved by different pilots, and for this survey we were unlucky to have selected a pilot who was not comfortable flying (very) low to the ground. In addition, it's more difficult to get the MD530 helicopter close to the ground than the Bell-206. For future surveys we will mount the modified sensor boom on the Bell-206.

In the western seed area, the Program Office emplaced 110 seeds in a geologically "challenging" environment. These consisted of a mix of 81 mm and 4.2-inch mortars, 105 mm high explosive anti-tank (HEAT)-rounds, and 105 mm and 155 mm projectiles. With a detection halo of 1.0 m, all items except 3 of 12 81 mm mortars were detected. Each detected anomaly was fit with a dipole model, and an apparent remanence metric was calculated and used to rank the anomalies by UXO likelihood. When using this ranking scheme 99% of the detected seed items occurred in the top 50% of the target declarations.

SNR was improved by a factor of about 18% compared to the previous generation system. The improvement occurred because of increased signal from the denser sampling of the magnetic field and reduced distortion in the signal and superior noise rejection from the new rotor-suppression algorithm.

2.0 INTRODUCTION

2.1 BACKGROUND

UXO contamination is a high priority problem for the Department of Defense (DoD). Recent DoD estimates of UXO contamination across approximately 1400 DoD sites indicate that 10 million acres are suspected of containing UXO. Because many sites are large in size (greater than 10,000 acres), the investigation and remediation of these sites could cost billions of dollars. However, on many of these sites only a small percentage of the site may in fact contain UXO contamination. Therefore, a number of wide area assessment (WAA) technologies, including helicopter Multi-sensor Towed Array Detection System (MTADS) magnetometry (HeliMag) technology, have been demonstrated and validated, both as individual technologies and as a comprehensive approach to WAA (Nelson et al., 2008; Nelson et al., 2005; Foley and Wright, 2008 a, b, c.).

HeliMag technology provides efficient low-altitude digital geophysical mapping (DGM) capabilities for metal detection and feature discrimination at a resolution approaching that of ground survey methods, limited primarily by terrain, vegetation, and structural inhibitions to safe low-altitude flight. The magnetometer data can be analyzed to extract either distributions of magnetic anomalies (which can be further used to locate and bound targets, aim points, and open burn/open detonation [OB/OD] sites), or individual anomaly parameters such as location, depth, and size estimate. The individual parameters can be used in conjunction with target remediation to validate the results of the magnetometer survey.

Developed by the NRL, HeliMag technology was transferred to Sky Research (SKY) via a Cooperative Research and Development Agreement (CRADA) in 2005. Since then, SKY has used the technology to characterize more than 100,000 acres at more than 20 sites, including the ESTCP WAA Pilot Program demonstration sites. During this technology transition process, several technical innovations were identified as having the potential to provide greater efficiency, broader applicability, and greater UXO detection capabilities. These innovations were completed, integrated with the HeliMag technology, and demonstrated at the former KPBR, in Albuquerque, New Mexico, as part of ESTCP project MM-0741, Next Generation HeliMag UXO Mapping Technology. This report documents the project activities, demonstration results, and performance evaluation for the project.

2.2 OBJECTIVES OF THIS DEMONSTRATION

The objectives of this demonstration were to improve HeliMag productivity and to expand HeliMag applicability. Specifically, these improvements were to be gained by a series of interconnected innovations:

- Improve data acquisition speeds through implementation of advanced data sampling and noise suppression methodologies (i.e. remove the sampling-based and filter-based limitations on survey speed)
- Enhance HeliMag detection by optimizing sensor configurations to ensure that the magnetic field is fully and optimally sampled, and improve noise suppression

techniques (e.g., implementation of the MD530F helicopter platform, revised filtering approaches) to maximize the SNR of targets of interest

- Enhance HeliMag data interpretation using automated detection and characterization algorithms (e.g., equivalent layer modeling, automatic magnetic dipole analysis/classification) to improve productivity and produce objective, repeatable (thus defensible) results
- Implement real-time data telemetry to remove the requirement to have a systems operator on board the aircraft, thereby increasing productivity (less weight provides an opportunity for more fuel and longer flight duration), expanding applicability (less weight provides a greater operational altitude range at existing fuel load conditions), and reducing risk (any aviation activity has an element of risk—removing the operator reduces the risk exposure accordingly).

2.3 REGULATORY DRIVERS

The U.S. Army Corps of Engineers (USACE) is the lead federal agency under the Formerly Used Defense Site (FUDS) program. USACE administers the FUDS Military Munitions Response Program (MMRP) program using DoD investigation and cleanup methods based on the U.S. Environmental Protection Agency (USEPA) Comprehensive Environmental, Response, Compensation, and Liability Act (CERCLA) process.

3.0 TECHNOLOGY

3.1 TECHNOLOGY DESCRIPTION

The next generation HeliMag system includes a helicopter-borne array of magnetometers (Figure 1), hardware, and software designed specifically to process data collected with this system and perform physics-based analyses on identified targets. Table 1 summarizes the system components. Brief descriptions of the components are provided in the following subsections, and a detailed description of each component is provided in Section 2 of the Demonstration Report (Billings and Wright, 2009a).

Table 1. Sky research next generation HeliMag technology components.

Technology Component		Specifications
Geophysical sensors		14 Geometrics 822 cesium (Cs) vapor magnetometers, 0.001 nanotesla (nT) resolution
Global Positioning System (GPS) Equipment		2 Trimble MS750 GPS receivers, 2-3 centimeter (cm) horizontal precision
Altimeters		1 Optech laser altimeter and 4 acoustic altimeters, 1 cm resolution
Magnetic attitude		Applied Physics 3-axis flux-gate
Data Acquisition System (DAS)		SKY DAS capable of data collection up to 400 Hz, 10 microsecond (μs) timing precision
Telemetry system	Ground antenna	MP-Tech Single Sector WFP0200508 120 Degrees Coverage
	Vehicle antenna	HD Communication Corp 5 dBi Omni HD24115
	Radio	Tranzeo TR600
	Amplifier	Luxul 1 W
Aircraft		Hughes MD530F helicopter

Figure 1. SKY next generation HeliMag system.
The sensor boom holds a linear array of 13 magnetometers spaced 0.75 m apart. A 14th sensor is temporarily mounted above the middle sensor to provide measured vertical gradient test data. The system is operated with an 'Experimental' category airworthiness certification.

3.1.1 Helicopter Platform

The MD530F helicopter is used to deploy the geophysical sensors, GPS equipment, altimeters, inertial measurement unit (IMU), DAS, and telemetry technologies listed in Table 1 and shown in Figure 1. Because the magnetic signal falls off quickly with distance, the helicopter is typically flown at survey altitudes of 1-3 m above ground level (agl). Onboard navigation guidance displays provides pilot guidance, with survey parameters established in a navigation computer that shares the real-time kinematic GPS (RTK GPS) positioning data stream with the DAS. Survey courses are plotted for the pilot in real time on the display. The sensor operator monitors presentations showing the data quality for the altimeter and GPS (along with the magnetometer data). Following each survey, the operator has the ability to determine the need for surveys of any missed areas before leaving the site.

3.1.2 Sensors and Sensor Configuration

The MTADS magnetic sensors are Geometrics 822A Cs vapor full-field magnetometers (a variant of the Geometrics 822). An array of 13 sensors is interfaced to the DAS. Sensors are evenly spaced at 0.75 m intervals at the same elevation on a 9 m Kevlar boom mounted on the helicopter. A 14th sensor is mounted 0.5 m higher and directly above the middle sensor.

3.1.3 Positioning Technologies

As in the initial Airborne Multisensor Towed Array Detection System (AMTADS) design, all data are positioned using two Trimble RTK GPS receivers with nominal accuracy of 2 cm horizontal and 4 cm vertical. Ancillary instrumentation records aircraft height above ground and attitude. A fluxgate magnetometer is used to allow for aeromagnetic compensation of the data as well as to provide redundant attitude information.

3.1.4 Telemetry System

Two antennas are used for the telemetry system. An omnidirectional antenna, an HD Communication Corp. antenna (referred to as the “whip”), is mounted on the helicopter and transmits data indicating the operational status of system components. An MP-Tech puck sector antenna, a multi-polarity diversity antenna with a vertical radiation pattern of 35° and a gain of 10 decibels (dB), is the ground station antenna and is manually pointed toward the helicopter during operation.

To monitor the link and test the remote link capabilities, computers on either end use VNC viewer software to allow remote computer control and to utilize the available bandwidth and data rates. Two laptops are used at the ground station, one for VNC to see the shared desktop in the helicopter and the other to monitor the signal strength of the wireless telemetry connected via a 12 volt (V) network switch.

3.1.5 Data Acquisition System

The SKY DAS uses a Linux operating system and logs magnetometer data at 400 Hz.

3.1.6 Data Processing

Data are downloaded via computer disks and uploaded via the Internet after each survey mission.

SKY's custom in-house software SkyNet is used to transcribe, filter, decimate, and position the airborne geophysical data. The output from SkyNet is either an ASCII xyz file or a Geosoft Oasis Montaj compatible database. Oasis is used to visualize the data and apply advanced processing where required. The SkyNET/Montaj combination facilitates data review, merging, correction, filtering, interpolation, and target picking while also providing an industry-standard data management system. A rotor noise suppression algorithm, described in Billings and Wright (2009a), suppresses rotor noise in the data without distorting the spatial response of any magnetic anomalies with overlapping frequency content.

3.1.7 Data Analysis

The gridded total magnetic field (TMF) image is used as a basis for selection of magnetic anomalies. The final product of a HeliMag site characterization survey is an anomaly density map. In order to aid in visualizing the distribution of metallic items across the areas, a density grid is computed using a 100 m radius neighborhood kernel that assigns anomaly densities in anomalies per hectare (1 hectare = 2.47 acres) to each cell in the grid (i.e., we sweep through a 100 m radius and count the number of targets and determine the area covered [in hectares]). We then calculate the density in anomalies/hectare and assign that value to the grid node. A radius of 100 m is suitable for detecting/delineating high-density areas that are indicative of UXO-contaminated impact areas. These grids are presented for visualization using a standard color stretch of 0-250 anomalies per hectare. This color stretch has been found to be ideal for recognizing and delineating "high concentration" areas that are indicative of extensive UXO contamination. High concentrations indicative of UXO contamination generally have anomaly densities greater than 200 anomalies/hectare.

3.2 TECHNOLOGY DEVELOPMENT

Development and testing of the first generation of helicopter magnetometry technology in general was supported by ESTCP (Nelson et al., 2005). The primary development objective was to provide a UXO site characterization capability for extended areas while retaining substantial detection sensitivity for individual UXO items. The system included data collection hardware in the form of a helicopter-borne array of magnetometers and software designed to process data collected with this system and to perform physics-based analyses on identified targets. The original NRL AMTADS sensor configuration is a linear array of seven sensors positioned using two GPS receivers as described in Wright et al. (2002). The initial sensor spacing was designed for nominal survey elevations of 3 to 5 m agl. Subsequent testing and demonstrations showed that nominal survey elevations of 1.5 to 2 m agl are regularly achievable.

3.2.1 System Component Development and Updates

Helicopter Platform

For the next generation HeliMag system, the Bell 206 Long Ranger (206L) was replaced with the MD530F helicopter to provide better power and maneuverability capabilities. The MD530F has

the best power/lift ratio of any small form-factor helicopter. This capability provides the pilot with better handling performance and allows for deployment in higher altitude settings.[1] The MD530F also has five blades (versus two for the Bell system), which provide increased operator control and lower vibration characteristics to support flying low-altitude missions. The rotor speed of the MD530F is also slightly higher than that of the 206L, providing some extra separation between the frequency of the magnetic rotor noise response and that of discrete UXO targets.

3.2.2 Sensors and Sensor Configuration

The modified sensor configuration of the next generation system represents a design optimized to achieve the objectives of this project through modeling and analysis conducted on existing data as discussed in Billings and Wright (2009b). This study evaluated the effects of geology and cultural features, coherent noise suppression alternatives, and dipole characterization processing to determine the optimal sensor spacing.

Based on the design study results, the following sensor configuration modifications were implemented:

- Modification of the existing boom to accommodate 13 sensors spaced 0.75 m apart
- Move the boom 0.5 m closer to the helicopter to reduce the amount of ballast required to offset the weight of the sensors
- Inclusion of a "reference" sensor close to the rotor-hub for coherent noise suppression. Following a shakedown test at the Former Lowry Bombing and Gunnery Range (FLBGR), the need for a reference sensor was obviated after the development of an intelligent noise-suppression algorithm.

3.2.3 Noise Suppression Algorithm

Rotor noise in the MD530F manifests itself at approximately 7.9 Hz (Billings and Wright, 2009). We could choose to suppress that using a low-pass filter with a cutoff of around 5 Hz. However, this places significant constraints on the survey velocity as a function of survey altitude: in particular, it is not possible to fly low and fast. To avoid these speed constraints, we apply a low-pass filter with a much less aggressive cutoff and rely on suppression of the rotor noise using one of two methods. For measured gradients we rely on the coherent noise rejection capabilities of vertically offset sensors. For the calculated gradients, we could use a reference sensor as per our previous analysis in Billings and Wright (2009). However, we have developed a more effective technique that does not require the reference sensor (see Appendix A in Billings and Wright, 2009). Essentially, the method calculates the period of the rotor noise and then computes a moving average of the rotor noise. The method accounts for small variations in the rotor noise period and fluctuations in the rotor noise amplitude. Additionally, this method is logistically less complex as it does not require an additional sensor and is not susceptible to errors due to competing signals measured at the reference sensor that are not due to the rotor.

[1] The increased maneuverability can result in larger heading errors so is not always an advantage.

3.2.4 Telemetry System

The telemetry system design was described in detail in Billings and Wright (2009a) and includes the components described in Section 3.1.4. Incorporation of telemetry into the data collection process provides real-time wireless communications between a ground-based sensor operator and the helicopter data system, enabling remote control of data acquisition without an onboard operator.

3.2.5 Shakedown Tests

Following the design study and initial telemetry system development and testing, the system components were assembled and installed. A shakedown test was conducted at the FLBGR near Denver, Colorado, in early June 2008 to demonstrate the functionality of the technical changes made to the HeliMag system and empirically confirm the findings of the sensor configuration optimization design study. The performance of the telemetry system components was also tested during the shakedown flights. The test activities and results are detailed in the Demonstration Report (Billings and Wright, 2009a) for this project and are not repeated here. Please refer to this document for additional information.

3.3 ADVANTAGES AND LIMITATIONS OF THE TECHNOLOGY

As with all characterization technologies, site-specific advantages and disadvantages exist that dictate the level of success of their application.

Advantages of HeliMag technologies include:

- The ability to characterize very large areas
- Lower cost as compared to ground-based DGM methods.

Limitations of HeliMag technologies include:

- As a WAA tool, it is not intended to detect individual UXO items.
- Site physical factors, such as terrain, soils, and vegetation, can constrain the use of the technology.

This page left blank intentionally.

4.0 PERFORMANCE OBJECTIVES

The performance objectives provide the basis for evaluating the performance and costs of the technology. For this demonstration, both primary and secondary performance objectives were established. Table 2 lists the performance objectives, criteria, and metrics used for evaluation. Discussion and analysis of the performance relative to each objective is provided in Section 8.

Table 2. Performance objectives and results.

Performance Objective	Metric	Data Required	Success Criteria
Ease of use	Efficiency and ease of use meets design specifications	Feedback from technician and pilot on usability of technology and time required	System efficient and easy to use
Georeference position accuracy	Comparison of validation target dipole fit analysis position estimates (in 3 dimensions) to ground truth	• Location of seed items surveyed to accuracy of 1 cm • Validation target dipole fit analysis position estimates (in 3 dimensions)	Target location estimates within 0.25 m radial horizontal error and 0.5 m vertical position error
Detection performance on seeded items	Percent detected (Pd) of blind-seeded items	• Location of seeded items • Prioritized dig list	Pd>0.9 for 60 mm and above
Detection performance compared to ground-based system	Comparison of target list with target lists generated from the full coverage data	Target lists of next generation system and ground-based systems for 60 mm mortar	Pd>0.9 for 0.03 ampere-meter squared (Am^2) anomalies (60 mm mortar) with probability of false alarm (Pfa) <0.5 (from ground-based)
Detection performance compared to AMTADS	Comparison of target lists from next generation HeliMag to that of the original AMTADS	• Target lists of next generation system and original AMTADS • Inflection point for both systems	Pd for next generation > Pd from AMTADS Inflection point (in total targets vs. detection threshold graph) for next generation lower than AMTADS
Telemetry link	Percentage of survey time during which the operator can view the DAS interface through VNC	Operator log	• Maintain link with helicopter for >80% of the data acquisition. • Interruptions limited to 15 minute durations.
Noise level (combined sensor/platform sources, post-filtering)	Accumulation of noise from sensors and sensor platforms calculated as the standard deviation of a 20 second window of processed data collected out of ground effect	20 second sample of data collected at high altitude (out of "ground effect")	<1nanotesla (nT) and <0.1 nT/m for calculated gradient
SNR improvement	Improved SNR relative to baseline HeliMag system	SNR of original and next generation sensor systems	Average SNR > original 7 sensor system for selected common anomalies

Table 2. Performance objectives and results (continued).

Performance Objective	Metric	Data Required	Success Criteria
Accuracy and noise of calculated vertical gradients	Gradients calculated by potential field operations on the total-field data and compared to the gradient measured by the one vertically offset sensor	Magnetic data over validation line	• Noise level of calculated gradient ≤ measured gradient • Better than 0.99 correlation between measured and calculated gradients
Accuracy of equivalent layer	Comparison of data predicted by equivalent layer at 2 m altitude compared to data predicted by upward continuation of ground-based data	Magnetic data over a portion of the site	Better than 0.95 correlation between equivalent layer and upward continued ground-based data at 2 m elevation
UXO parameter estimate repeatability	Size and dipole angle estimates of the calibration items consistent	Daily calibration data	• Size <50% (standard deviation) • Angle relative to Earth's field < 20º (standard deviation)
Operating parameters (altitude, speed, production level)	Values calculated using average and mean statistical methods to compute each parameter.	Statistics extracted from databases (altitude/speed) and field data logs (production level)	1-3 m agl; 10-30 m/s (20-60 knots); 300 acres/day
Rotor noise suppression algorithm at high speed	Comparison of high and low-speed results over validation line targets to verify correct operation of rotor noise suppression algorithm when the signal frequency overlaps the rotor noise frequency	Data acquired over validation line	Fit error of dipoles on validation-line survey collected at high-speed within 5% of low-speed data
Data density/point spacing	• Along track: (# of sensor readings/second) / airspeed • (Across track: sensor line spacing = 0.75 m)	Statics derived from survey databases (along track density) and sensor configuration (cross-track sensor spacing)	0.1 -0.3 m along-track (0.2 m at 100 Hz sample rate, 20 m/s ground speed) 0.75 m cross track
Survey coverage	Surveyed acres/planned survey acres	• Actual # acres surveyed • Planned # of survey acres	>0.95 of planned survey area

5.0 SITE DESCRIPTION

5.1 SITE LOCATION AND HISTORY

The Former KPBR is a World War II (WWII)-era former military training facility located about 2 miles west to 18 miles northwest of the western city limits of Albuquerque, New Mexico. Within the 15,246 acre FUDS, ESTCP established a 6500 acre demonstration sub-area for the WAA Pilot Program (Figure 2). Results from the data analysis for the WAA Pilot Program confirmed the presence of three precision bombing targets (N2, N3, and New Demolitions Impact Area [NDIA]), a simulated oil refinery target (SORT), and several additional areas of interest. These areas are all located within the northern section of the WAA site shown on Figure 2. Currently the study area is undeveloped. Portions are planned for commercial or industrial development within the next decade, and airport expansion into these lands is possible.

5.2 SITE GEOLOGY

The soils within the survey area are deep, well-drained homogeneous sandy loams formed on loess parent material with low magnetic mineral content. However, to the east of the study area, several volcanic cinder cones rise about 300 ft above the surrounding terrain, and there are some magnetic protrusions present across the site, most likely associated with the volcanics. The vegetation is short-grass prairie and cultivated fields with very few trees and shrubs that would pose a constraint to low airborne operations.

5.3 MUNITIONS CONTAMINATION

Munitions known or suspected to have been used on the site include 100 lb practice bombs and 250 lb high-explosive (HE) bombs. Target N2 is documented as a 160-acre quarter-section containing a circular night bombing target including power plant, underground cables, floodlights, and target circle. Target N3 is documented as being within a 320-acre half-section near the northwest corner of the study area. This target was cleared in 1952, and large pits within the area have been hypothesized as OB/OD areas. The NDIA target area is a target circle. The SORT area was documented in the Archive Search Report (ASR) with location unknown, in the current conceptual site model (CSM) (Versar, 2005). The surveys conducted under the WAA Pilot Program confirmed its presence. These areas are shown on Figure 2.

Documented ordnance present on the site surface within the study area includes the following:

- M38A2 100 lb practice bombs and spotting charges
- M85 100 lb practice bombs and spotting charges
- 250 lb general purpose HE bombs.

Aircraft flares also were reportedly dropped. Information in the ASR indicates that a single 250 lb HE bomb was dropped “unofficially” by each trainee bombardier upon graduation from the training course, probably at the NDIA target area east of the N2 target area.

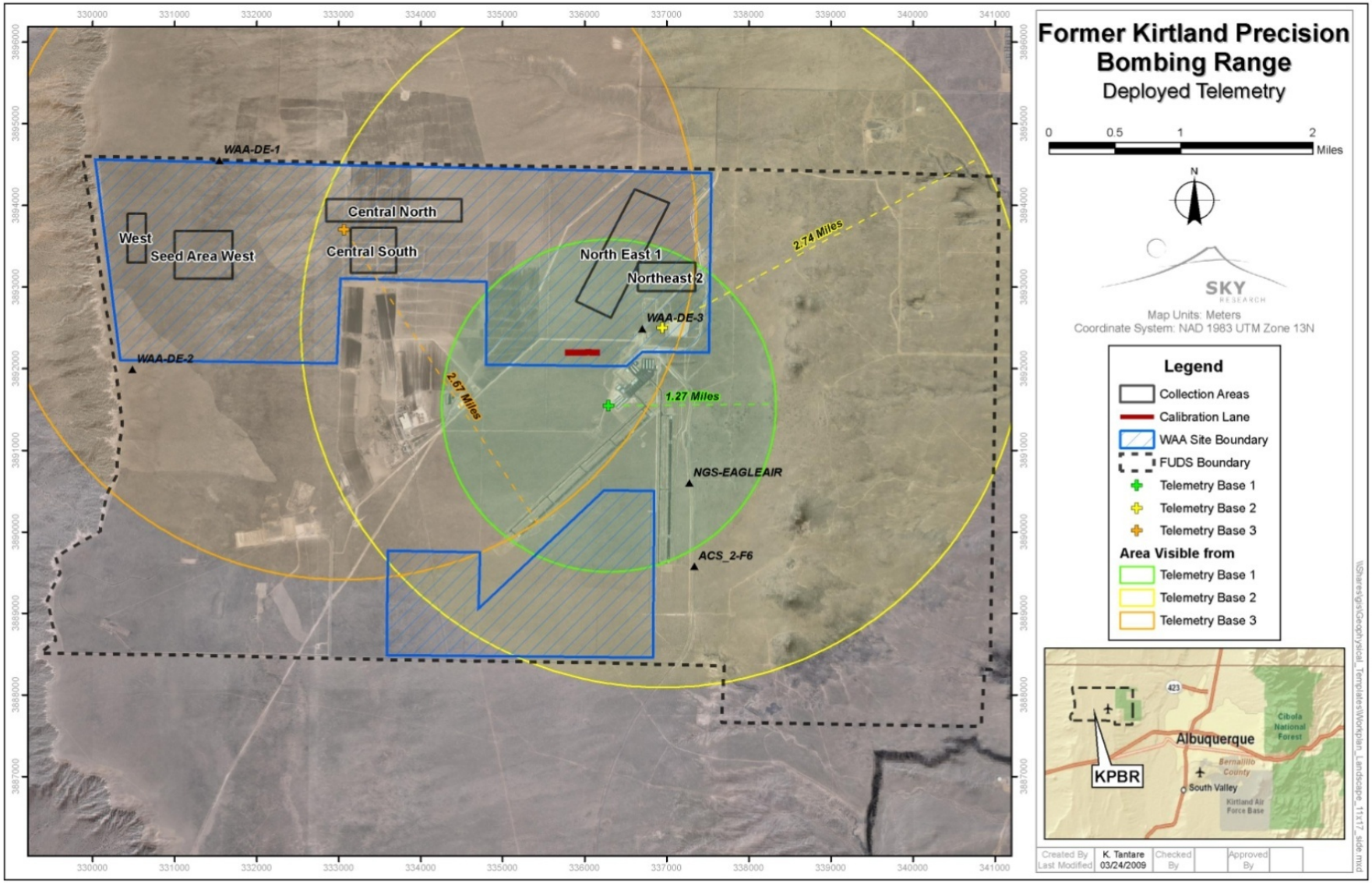

Figure 2. Former Kirtland Precision Bombing Range with HeliMag 2009 test areas (black outline) superimposed on HeliMag data collected in 2005 (WAA boundary–blue outline).

6.0 TEST DESIGN

In 2005, the WAA Pilot Program selected the Former KPBR as one of the demonstration sites. For that demonstration, two parcels totaling 5000 acres on either side of Double Eagle Airport were chosen. Results from data analysis from the WAA Pilot Program confirmed the presence of three precision bombing targets (N2, N3, and NDIA), the SORT, and several additional areas of interest. The area surveyed using the Next Generation HeliMag system lies to the North of the Double Eagle Airport. Approximately 560 acres was planned to be surveyed, including the areas previously surveyed with ground-based systems and parts of the SORT and NDIA bombing targets (Figure 2). Conducting the demonstration at KPBR allowed comparison of the results of this system configuration with results from previous HeliMag surveys conducted under the WAA and other demonstrations, including full-coverage ground-based surveys.

6.1 CONCEPTUAL EXPERIMENTAL DESIGN

For this demonstration, the next generation HeliMag system was used to survey approximately 586 acres configured to encompass a subset of the areas surveyed as part of the Pilot Program. The extent of the planned survey area is shown in Figure 2 and comprises the following six areas:

- North-central survey area (118 acres) covering three full-coverage ground-based grids and part of the SORT area. The area covered with the ground-based grids was used for seeding.
- South-central survey area (79 acres) covering two full-coverage ground-based grids. The area covered with the ground-based grids was used for seeding.
- Northeast 1 survey area (190 acres) covering three full-coverage ground-based grids and part of the NDIA area.
- Northeast 2 survey area (58 acres) covering two full-coverage ground-based grids.
- Western seed area (105 acres) established for testing of Battelle's electromagnetic (EM) helicopter array.
- Western ground-coverage area (36 acres) overlying a full-coverage grid collected by Science Applications International Corporation (SAIC).

All the areas surveyed for this demonstration also overlapped with areas surveyed using the AMTADS helicopter system in 2005 (Nelson et al., 2005), and most overlapped with 10 areas that were surveyed on the ground in full coverage mode by the Vehicular Simultaneous Electromagenetic Induction and Magnetometer System (VSEMS) (Seigel, 2008).

The ESTCP Program Office blind-seeded part of the area with 60 and 80 mm mortars. The area reserved for seeding overlapped three of the full-coverage grids. In addition, a 100-acre seeded area was surveyed that had already been established by the Program Office for testing of the Battelle airborne EM array. This area was seeded with 81 mm and 4.2-inch mortars, 105 mm and 155 mm projectiles, and 105 mm HEAT rounds.

Because previous HeliMag, AMTADS, and ground-based systems have been demonstrated at the site, overlap of survey areas allowed for comparison of the datasets as an effective mechanism for evaluating the next generation system performance.

6.2 SITE PREPARATION

No site preparation (i.e., vegetation removal, site clearance, etc.) was required.

ESTCP emplaced blind seeded targets in the north-central survey area and south-central survey area where ground-based grids were located. The ground truth data was protected from the performers until after the data analysis was complete.

6.3 SYSTEM SPECIFICATION

A description of the system components is provided in Section 3.1, with additional detail provided in the Demonstration Report (Billings and Wright, 2009a). The data collection flight parameters specified for the demonstration are presented in Table 3.

Table 3. Flight parameters for data collection.

Parameter	Specifications
Flight speed average	40 knots (20 m/second [m/s])
Flight speed range	20 to 60 knots (10 to 30 m/s)
Altitude	1 to 3 m agl
Across track spacing	0.75 m
Flight line separation	7.0 m separation to provide 40% overlap between adjacent passes
Along track density	0.2 m (at 100 Hz sample rate, 20m/s ground speed)

6.4 DATA COLLECTION

The field data collection program ran from initial mobilization on March 14 to demobilization on March 20, 2009. Figure 3 shows the areas surveyed in reference to the previous surveys. Initial testing began on March 16 and data acquisition occurred from the 17th to the 20th. There were minor delays on each of the first two data acquisition days due to reconfiguration of the boom mounting hardware. Additionally, poor GPS quality on March 18 resulted in more reflies than are typically required for HeliMag surveys. Discounting time lost for these delays, a total of 586 acres was surveyed in approximately two survey days.

The data processor performed the initial review of the geophysical data following each survey day. As needed, adjustments were made to the field operations or data processing to ensure quality data collection. The initial review of geophysical (magnetometry) data was performed to ensure that the data were within a reasonable range (35,000–75,000 nT), free from dropouts/spikes, and timing errors and otherwise appear to be valid. Invalid data were removed and, where appropriate, requests for re-flights passed to the acquisition team.

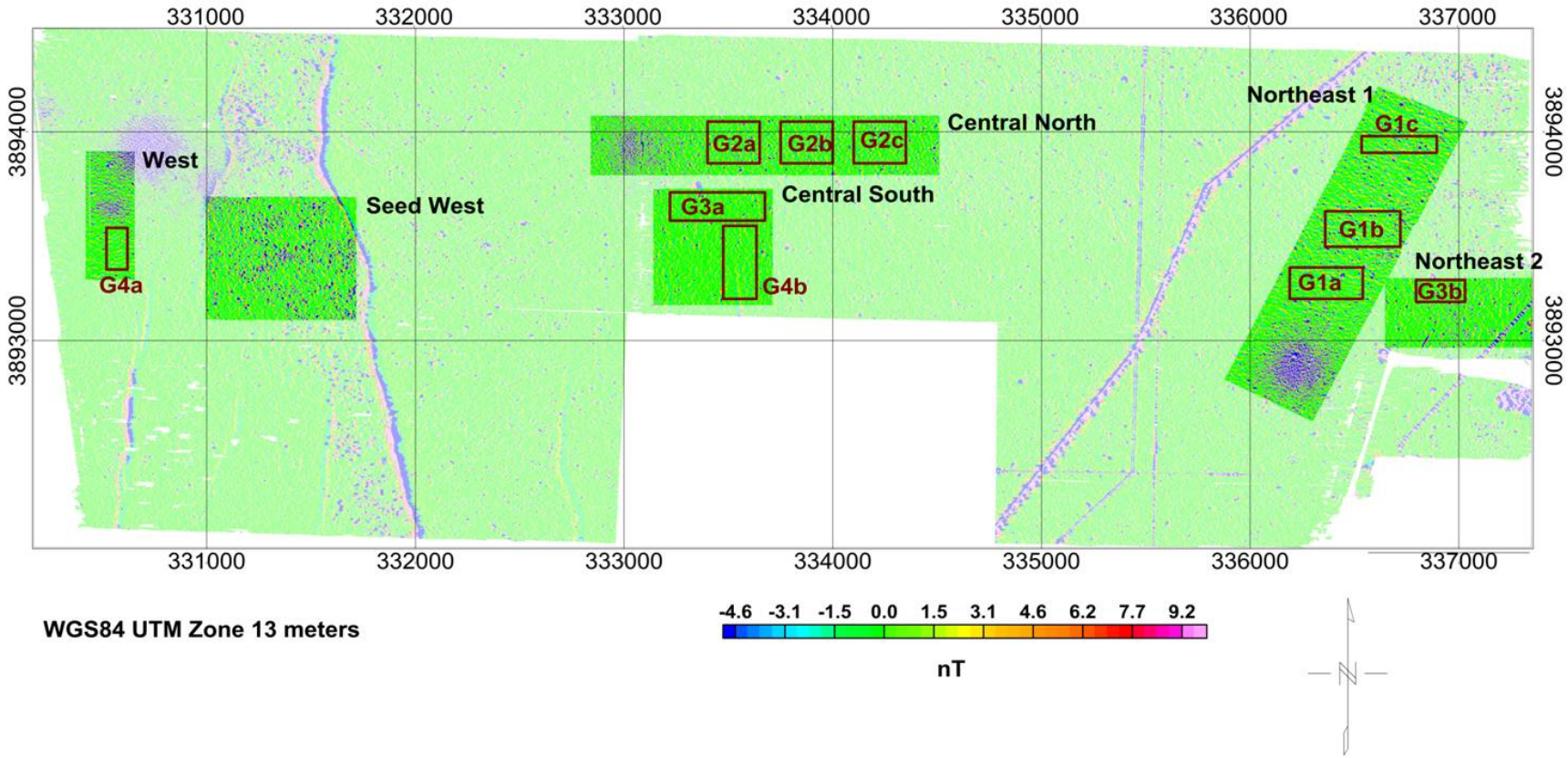

Figure 3. Overview of survey data collected.
The areas with opaque palettes were collected with the 13 sensor HeliMag configuration. The large semi-opaque palette is the AMTADS 2005 data set, and the boxes outlined in red represent areas that were surveyed with a ground-based towed magnetometer array in 2005.

The initial review of positional data involved checking line profiles for position dropouts/spikes. A GPS fix quality indication was recorded as part of the GPS data string. Any data tagged with a fix status that indicated the GPS was not operating in "RTK-fix" mode (nominally 2 cm level accuracy) were rejected automatically. After the initial data review described above, the data underwent a site-specific processing procedure for sensor data filtering, gridding, and visualization that was developed based on preliminary analysis of the validation and initial survey results.

In addition to the quality checks and initial data review described above, we expended significant effort understanding and mitigating the dominant intrinsic noise source of the system which originates in the rotor-hub. It is an especially problematic noise-source because, when flying fast and low, the frequency range of the noise (7.8 Hz) overlaps with the frequency content of near-surface metallic items. Thus, it can't be suppressed with a low-pass or notch filter without distorting the spatial structure of the underling signals of interest. The rotor-suppression algorithm that was developed and applied to the FLBGR test-data often failed when applied to the Kirtland data. We thus sought to develop a more reliable algorithm by studying the characteristics of the rotor-noise. The findings are presented in detail in Section 4.5.2 of the Demonstration Report (Billings and Wright, 2009a) and are not further expanded upon here.

At our final sample rate of 100 Hz, the survey speeds of 15–25 m/s (20–50 knots per hour [kts]) resulted in down-line data spacing of 0.15-0.25 m and 0.75 m crosstrack spacing. The sample density relative to the performance objective is further discussed in Section 8.10. This performance largely met our objective of 0.1-0.3 m along-track (0.2 m at 100 Hz sample rate, 20 m/s ground speed) and 0.75 m cross-track density.

The data for the demonstration comprise raw data and processed data products (target list and magnetic data). Images and target density estimates were then derived from these products.

6.5 VALIDATION

Detection performance was scored based on the seeded items, and additional performance measures were based on comparison with the data collected during previous AMTADS and ground-based demonstrations. Detailed results and analysis of the performance are provided in Section 8.3.

7.0 DATA ANALYSIS AND PRODUCTS

This section provides a broad outline of the major analysis steps used to produce the data products.

7.1 PREPROCESSING

The raw data were transcribed from their native data file formats into ASCII xyz files using SkyNet. At this point, the geophysical data were subjected to a lowpass/notch filter, decimated to a sample rate of 100 Hz, and assigned 3D positions based on the GPS master antenna position, aircraft attitude, and the system geometry. Because the geophysical and position data were collected asynchronously, they were aligned with respect to their time of applicability. This was performed automatically during the merge process based on highly precise time stamps associated with each data channel.

7.2 TARGET SELECTION FOR DETECTION

The gridded TMF image as well as the "analytic signal" (i.e., total gradient) were used as the basis for selection of magnetic anomalies. Geosoft's peak detection routine was applied to the analytic signal grids to automatically select targets with response amplitudes significantly above the nominal geologic noise. The SKY analyst used a cutoff threshold of 4 nT/m (SNR = 8) for the auto-detection process and augmented the target list by selecting and deselecting anomalies based on the TMF image.

Recently, SKY has developed analysis techniques to extract more information from the data and improve delineation of potentially hazardous areas. These techniques involve refining the target lists based on parameters derived from the dipole fit analysis. This process is described in detail in Section 7.3.

7.3 PARAMETER ESTIMATES

Each selected anomaly is subjected to a dipole fit analysis to derive features (e.g., dipole size, orientation, and position). The analysis software extracts sensor data points associated with each selected target. Each sensor reading is an input datum used in a seven-parameter, iterative calculation to derive the parameter values that describe a dipole model that best fits the observed data. These parameters include dipole position (3 dimensions), dipole angle (2 dimensions), dipole magnitude (size), and an offset parameter to account for any bias in the magnetometer data.

7.4 CLASSIFIER AND TRAINING

The dipole parameters derived from the target picking step are then classified using the apparent magnetic remanence metric (Billings, 2004). Items used to calculate apparent remanence were 60 mm and 81 mm mortars (small ordnance), 105 and 155 mm projectiles (medium ordnance) and a 100 lb bomb (large ordnance). If the apparent remanence was less than 70%, then the item was assigned to the corresponding class (e.g., small ordnance) whereas if larger, it was placed in a low confidence UXO class (e.g., low confidence small ordnance). Any items with a depth greater

than 3.95 m are assigned to a "low confidence metallic" class, while items with failed fits are placed in a "can't analyze category." The target list is then ordered by apparent remanence, with smaller values representing items with a higher likelihood of being a UXO. Final outputs from this step are an ASCII formatted target list providing target identification (ID), refined position and associated dipole parameters, and target classification declarations.

7.5 DATA PRODUCTS

7.5.1 Raw Data

The raw data is supplied in Geosoft XYZ format, which consists of an ASCII file with individual data collection lines delineated by a line header NNNNNNN.s, where s is the sensor number. The columns are:

- *Time (seconds):* The GPS time of the magnetometer measurement
- *Easting (meters):* Easting of measurement in NAD83 datum
- *Northing (meters):* Northing of measurement in NAD83 datum
- *Elevation (meters):* Height above ellipsoid of the measurement in NAD83 datum
- *h_agl (meters):* Estimated height of measurement above the ground
- *Sensor_Number:* Sensor number, 1 is far left up to 13 on the far right and with 14 the central sensor that is 0.5 meters higher
- *Mag_Raw (nT):* Raw magnetic data (after application of rotor suppression algorithm, but before aeromagnetic compensation and geology removal)
- *mag_full_fin (nT):* Compensated magnetic data
- *Mag_demedian_fin (nT):* Compensated and high-pass filtered magnetic data.

7.5.2 Target Lists

These were provided in Microsoft Excel format with the following columns:

-
- *Target: A unique label identifying the anomaly number*
- *X (meters): Easting in NAD83 datum*
- *Y (meters): Northing in NAD83 datum*
- *Depth (meters): Estimated depth below the ground of the anomaly*
- *Elevation (meters): Estimated height above ellipsoid of the anomaly*
- *dx (meters): Difference between the original estimate of the easting and the refined estimate returned by the dipole model*
- *dy (meters): As for dx but for the northing*
- *MagMin (nT): Minimum value of magnetic data about anomaly*

- *MagMax (nT): Maximum value of magnetic data about anomaly*
- *MagAmp (nT): Difference between anomaly maximum and minimum*
- *Moment (Am2): Magnitude of fitted dipole moment*
- *Azimuth (degrees): Azimuth of dipole moment measured clockwise from magnetic north*
- *Dip (degrees): Dip of dipole measured below the horizontal (0 for a horizontal dipole)*
- *CorrCoeff: Correlation coefficient between observed and predicted data*
- *NumData: Number of data points that constrain the dipole fit*
- *Angle (degrees): Angle between the Earth's field and the fitted dipole moment*
- *Fit: Indication of whether the fit is acceptable or not*
- *Comment: Comment regarding the fit (typically auto-generated)*
- *Best Item: Item with lowest magnetic remanence*
- *Remanence (%): Apparent remanence of the fitted dipole moment.*

This page left blank intentionally.

8.0 PERFORMANCE ASSESSMENT

The results achieved during the technology demonstration are presented in Table 4, and a summary of the results and data analysis performed in support of the performance assessment is provided.

Table 4. Performance objective results.

Performance Objective	Confirmation Method	Expected Performance	Performance Achieved
Ease of use	Efficiency and ease of use meets design specifications	System efficient and easy to use	Met with qualifications (see text)
Georeference position accuracy	Comparison of validation target dipole fit analysis position estimates (in 3 dimensions) to ground truth	Target location estimates within 0.25 m radial horizontal error and 0.5m vertical position error	Met Standard deviation of location error was 23 and 24 cm for central and west seed areas and 7 cm for validation line objects. Vertical error standard deviations for central and west were 29 and 21 cm and for validation line were <23 cm.
Detection performance on seeded items	Pd of blind-seeded items	Pd > 0.9 for 60 mm and above	Met for 81 mm on central seed area but not on 60 mm • Pd = 100% for 81mm • Pd = 23% for 60mm Met for all projectiles on western seed area except 81 mm • Pd = 98% for all (except 81 mm) • Pd = 58% for 81 mm
Detection performance compared to ground-based system	Comparison of target list with target lists generated from the full coverage data	Pd > 0.9 for 0.03 Am^2 anomalies (60 mm mortar) with Pfa < 0.5 (from ground-based)	Not evaluated as ground-based data were high-pass filtered using significantly different parameters than the airborne data.
Detection performance compared to AMTADS	Comparison of target lists from next generation HeliMag to that of the original AMTADS	Pd for next generation > Pd from AMTADS Inflection point (in total targets vs. detection threshold graph) for next generation lower than AMTADS	• Pd < 2005 AMTADS data due to altitude differences, but >simulated AMTADS data (7 sensors, low-pass filtered) • Pd against seeded targets > for simulated AMTADS data • Inflection points comparable (when presented in terms of SNR)
Telemetry link	Percentage of survey time during which the operator can view the DAS interface through VNC	Maintain link with helicopter for >80% of the data acquisition—Interruptions limited to 15 minute durations	Met • Telemetry link maintained for > 95% of the time. • Worst performance had telemetry link maintained for 70% of a flight (< 5 minute interruption)

Table 4. Performance objective results (continued).

Performance Objective	Confirmation Method	Expected Performance	Performance Achieved
Noise level (combined sensor/platform sources, post-filtering)	Accumulation of noise from sensors and sensor platforms calculated as the standard deviation of a 20 sec window of processed data collected out of ground effect	<1 nT and < 0.1 nT/m for calculated gradient	Met • Noise standard deviation <0.42 nT on all sensors (probably closer to 0.1 to 0.2 nT) • Standard deviation for both calculated and measured gradients <0.1 nT/m
SNR improvement	Improved SNR relative to baseline HeliMag system	Average SNR > original 7 sensor system for selected common anomalies	Met Factor of 1.17 improvement over 2005 AMTADS data and 1.68 over simulated AMTADS data (same altitude)
Accuracy and noise of calculated vertical gradients	Gradients calculated by potential field operations on the total-field data and compared to the gradient measured by the one vertically offset sensor	• Noise level of calculated gradient ≤ measured gradient • Better than 0.99 correlation between measured and calculated gradients	Met, correlation coefficient 0.997
Accuracy of equivalent layer	Comparison of data predicted by equivalent layer at 2 m altitude compared to data predicted by upward continuation of ground-based data	Better than 0.95 correlation between equivalent layer and upward continued ground-based data at 2 m elevation	Not evaluated due to limited data fit with an equivalent layer
UXO parameter estimate repeatability	Size and dipole angle estimates of the calibration items consistent	• Size <50% • Angle relative to earth's field <20º	Met • Size <30% • Angle <10º.
Operating parameters (altitude, speed, production level)	Values calculated using average and mean statistical methods to compute each parameter.	1-3 m agl; 10-30 m/s (20-60 knots); 300 acres/day	• Altitude = 1.6 – 2.0 m (depending upon survey area) • Speed = 15 – 25m/s (depending upon survey area) • Production rate = 290 acres/day
Rotor noise suppression algorithm at high speed	Comparison of high and low-speed results over validation line targets to verify correct operation of rotor noise suppression algorithm when the signal frequency overlaps the rotor noise frequency	• Planed: Fit results of dipoles on validation-line survey collected at high-speed within 5% of low-speed, low-pass filtered data • After survey: Used visual assessment of low-pass and rotor noise suppressed data on validation lane	Met, using semiquantitative criteria
Data density/ point spacing	• Along track: (# of sensor readings/sec/airspeed • Across track: sensor line spacing = 0.75 m	• -0.3 m along-track (0.2 m at 100 Hz sample rate, 20 m/s ground speed) • 0.75 m cross track	• 0.15 – 0.25 m along track • 0.75 m cross track (worst case)
Survey coverage	Surveyed acres/planned survey acres	>0.95 of planned survey area	Met, 0.99

8.1 EASE OF USE

"Ease of use" is a qualitative performance metric that we assume is met when the survey is performed with satisfactory results in the time period predicted, as was the case for this demonstration. With the exceptions of the new helicopter platform (MD350F) and the implementation of a telemetry system to remove the system operator from the aircraft, this deployment was very similar to previous demonstrations of the HeliMag technology.

Although the telemetry system worked well, there were some software glitches that made the utilization of this system less than seamless, necessitating occasional rebooting of the data acquisition system. These problems were noncritical and will be resolved prior to any subsequent deployments.

SKY has performed a number of surveys with the MD350F. However, this was the first opportunity to test and compare the performance of this aircraft with that of the original Bell 206L platform. During the survey the pilot experienced difficulty flying as low as the previous survey. After modifications were made to the boom mounting system, a satisfactory survey altitude was achieved.

8.2 GEOREFERENCE POSITION ACCURACY

The positions estimated from the validation lane are shown in Figure 4. The maximum position error is 28 cm in easting and 34 cm in northing, with a mean-square error of 9.7 cm easting and 12.7 cm northing. Several of the items appear to be consistently biased (e.g., the 100-lb bomb is about 20 cm biased in both easting and northing). Because this bias is consistent for each target, (and not consistent for each survey pass) we assume that the error is related to the ground truth measurement of the target position. After correcting for the bias in each validation item, the mean-square error falls to 4 cm in rasting and 5.6 cm in northing, with maximum errors of 11 cm in easting and 19 cm in northing.

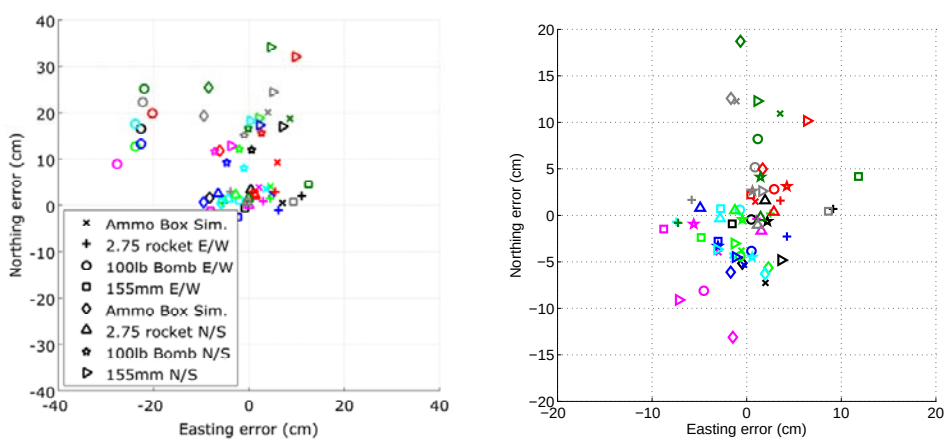

(a) Raw comparison (b) After adjusting for bias

Figure 4. Estimated locations of items on the validation lane for all 4 days with the lane flown twice per day.

In (a) the raw results are shown while in (b) the results are shown after adjusting for bias. The results are shown in different colors for each pass over the validation line.

8.3 DETECTION PERFORMANCE

The detection performance was assessed by analysis of three scenarios. Where available, we used vehicular towed magnetic array (ground) as ground truth to compare and contrast the "old" HeliMag (AMTADS) data set collected in 2005 with the data collected as part of this demonstration. In areas where we have only the 2005 and 2009 airborne data we compare and contrast the relative performance of the two systems. Finally, we report the detection performance of the next generation HeliMag system against blind seeded targets. We present the analysis for only the last scenario here, with the first two described in detail in the associated demonstration report (Billings and Wright, 2009a).

8.3.1 Scenario 1: Ground Vehicle, 2005 AMTADS and 2009 HeliMag Data

See Billings and Wright (2009a).

8.3.2 Scenario 2: 2005 AMTADS and 2009 HeliMag Data

See Billings and Wright (2009a).

8.3.3 Scenario 3: Detection of Blind Seeded Targets

8.3.3.1 60 and 81 mm Mortars in the North-Central Seed Area

The ESTCP program office arranged for the blind (to SKY) seeding of 80 targets in the north-central area. These were equally divided between 81 and 60 mm mortars. After processing of the geophysical data, the SKY analyst manually selected targets from the gridded results. Each target was analyzed using the SKY dipole fit algorithm to derive six parameters that define the position, orientation, and size of the best fit dipole as well as a seventh parameter that is a measure of the goodness of fit of the modeled dipole to the observed data. These parameters were used to refine the target position and classify the target. Each target was assigned one of the classes provided in Table 5.

Table 5. Classes used in the interpretation of the seed area data.

Class #	Class Name	Classification criterion
1	Potential small UXO	Apparent remanence less than 70% and best matched to a 60 or 81 mm mortar
2	Potential medium UXO	Apparent remanence less than 70% and best matched to a 105 or 155 mm projectile
3	Potential large UXO	Apparent remanence less than 70% and best matched to a 100 pound bomb
4	Low confidence small UXO	Apparent remanence greater than 70% and best matched to a 60 or 81 mm mortar
5	Low confidence medium UXO	Apparent remanence greater than 70% and best matched to a 105 or 155 mm projectile
6	Low confidence large UXO	Apparent remanence greater than 70% and best matched to a 100 pound bomb
7	Low confidence metal	Dipole depth greater than 3.95 m (regardless of apparent remanence)
8	Poor dipole fit	Dipole fit correlation coefficient <.8

A total of 982 targets was classified and submitted to the Institute for Defense Analyses (IDA) via the ESTCP Program Office for scoring. An emplaced target was declared detected if a submitted target position was within a 1.5 m halo of the emplaced target position. The scoring results as provided by IDA are presented in Table 6.

Table 6. Scoring results as generated by IDA for the seed targets in the north-central area.

Halo Radius	UXO Type	Total # Seeds	# Seeds Detected	Pd	Mean (Xi)	Mean (Yi)	Sdev (Xi)	Sdev (Yi)	Mean (dist)	Std Dev (dist)
0.5 m	All	80	33	0.41	0.03	-0.07	0.23	0.16	0.27	0.10
0.5 m	81 mm	40	29	0.73	0.01	-0.07	0.23	0.16	0.26	0.10
0.5 m	60 mm	40	4	0.10	0.14	-0.05	0.28	0.22	0.33	0.12
1 m	All	80	49	0.61	0.08	-0.14	0.32	0.30	0.40	0.23
1 m	81 mm	40	40	1.00	0.11	-0.08	0.32	0.24	0.37	0.21
1 m	60 mm	40	9	0.23	-0.06	-0.39	0.29	0.38	0.55	0.26
1.5 m	All	80	49	0.61	0.08	-0.14	0.32	0.30	0.40	0.23
1.5 m	81 mm	40	40	1.00	0.11	-0.08	0.32	0.24	0.37	0.21
1.5 m	60 mm	40	9	0.23	-0.06	-0.39	0.29	0.38	0.55	0.26

All the targets that were detected were within a 1 m halo of the emplaced target position and 67% of the detected targets were within a 0.5 m halo. Of the 81 mm targets, 100% were detected with a mean miss distance of 0.37 m. Only 23% of the 60 mm targets were detected, with a mean miss distance of 0.55 m. Overall this performance is better than earlier documented detection performance against 81 mm. In 2003 a test was performed with similar site conditions at the Isleta Pueblo. For this test less than 50% of the 81mm targets and only 20% of the 61 mm targets were detected (Tuley and Dieguez, 2005).

In the left panel of Figure 5 we show the SNR levels of each of the targets. The signal levels are calculated by sampling the analytic signal (AS) grid at the ground truth positions of the emplaced targets. The noise was calculated as the standard deviation of 200 randomly positioned AS samples (identified by the analyst as non-anomalous). The solid black horizontal line at SNR=8 shows a reasonable cut off threshold, below which targets become very difficult to detect. As described earlier, we can use the recent HeliMag data to simulate the original AMTADS configuration and filter process. On the right side of Figure 5, we can see that the seeded target SNR values are significantly reduced for the simulated AMTADS data, and using the same threshold it is apparent that the detection performance would have been significantly less.

As mentioned above, the target selections were performed manually by the SKY analyst. In practice the analyst uses an auto-detection routine with a conservative cutoff threshold—in this case, the threshold was 4 nT/m (SNR = 8). The analyst then augments the auto-detected target list with manual additions and deletions. This explains how we can detect some targets that are apparently below the auto-picker cutoff threshold as well as how some missed targets have significantly greater SNR values than some detected targets.

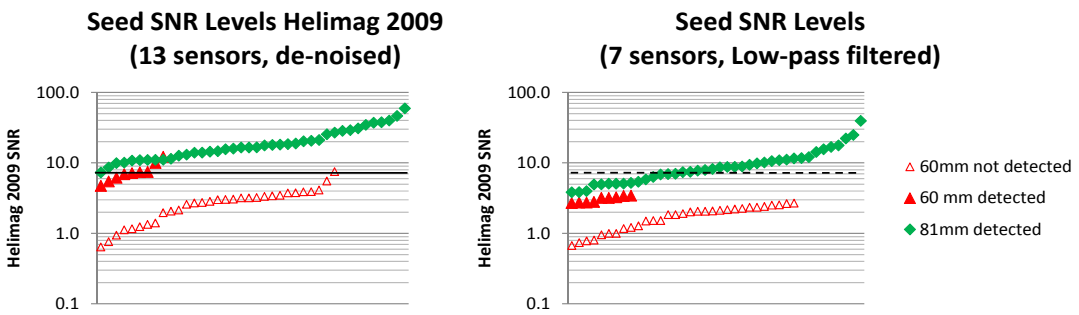

Figure 5. Seeded target SNRs for the HeliMag system (left panel) and simulated AMTADS system (right panel).

Signal levels were determined by sampling the analytic signal grids at the seeded ground truth positions, and noise levels were determined as the standard deviation of 200 samples taken in visually quiet positions distributed throughout the north-central area. The horizontal black line marks the auto-picker cutoff threshold used by the analyst.

We can use the automatic target detection routine to sample targets at a series of different thresholds and produce a pseudo receiver operating characteristic (ROC) curve that shows the detection performance as the threshold moves down into the noise (bottom left panel of Figure 6). Because we are not attempting to discriminate and do not have an independent measure of false alarms, we simply show the number of detected anomalies that are required to attain a given Pd. At a Pd of 0.6 there is a significant inflection point in this curve where the number of detections required to improve the Pd increases dramatically. In the right side of Figure 6, we plot the Pd and the number of detections as a function of SNR threshold for the HeliMag system (upper panel) as well as for the simulated AMTADS (lower panel). The solid vertical black line on the HeliMag 2009 chart indicates the cutoff threshold of 8 used by the analyst. The dashed black line on the simulated AMTADS chart shows the position of an equivalent cutoff threshold. The tighter sensor spacing afforded by the 13-sensor system combined with the new de-noising algorithm results in a higher detection rate at similar SNR thresholds.

Although the Pd on these curves reaches 1, in practice the upper Pd limit is constrained by the noise. Below a threshold of 5, the additional number of total detections associated with gains in Pd rises dramatically.

In an attempt to refine target lists and separate targets of interest from targets due to other sources (such as geology, and non-UXO-like metal debris) we use the dipole fit derived features to classify each anomaly. Without an extensive ground truth program, we were not able to assess the performance using standard Pd versus Pfa ROC curves. However, we can infer the efficacy of the classification approach by comparing the classification distribution for the seeded targets that were detected with the distribution for the entire set of anomalies (Figure 7). All the detected anomalies were classified correctly as small UXO, and only 16% of these were “low confidence” declarations. Of all of the anomalies reported, only 36% were declared to be small UXO (22% low confidence). These results imply that dipole fit analysis and classification is a useful tool to reduce the total number of targets and refine the target lists.

Seed Detection Analysis:

Automated 'peak detection' threshold range = 0.5 to 50 nT/m (analytic signal)

Helimag 2009 'noise' = 0.5 nT/m
Simulated AMTADS 'noise' = 0.4 nT/m

SNR threshold = peak analytic signal/noise

80 blind seeded targets:
- 40 60mm mortars
- 40 81mm mortars

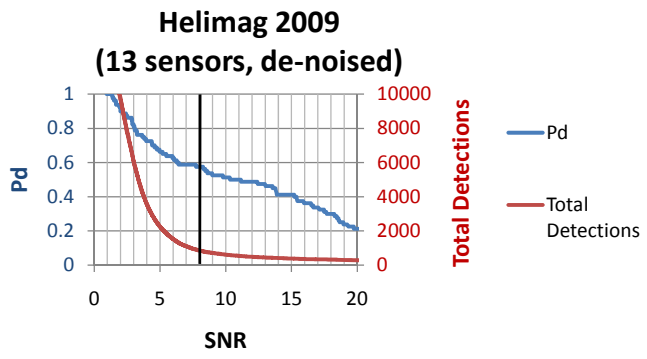

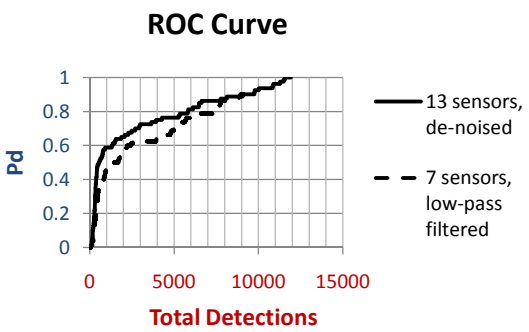

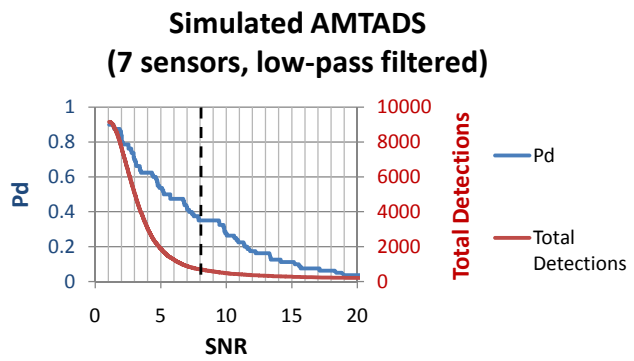

Figure 6. Pseudo ROC curves for seeded targets (bottom left), and graphs of total detections and Pd plotted as a function of SNR cutoff threshold for the HeliMag data (upper right) and simulated AMTADS data (lower right).
The vertical black lines mark the auto-picker cutoff threshold.

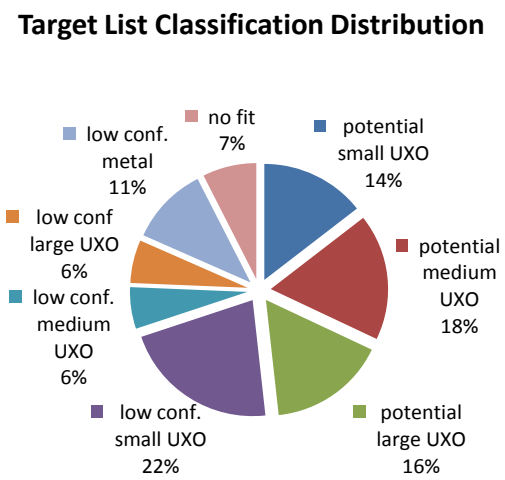

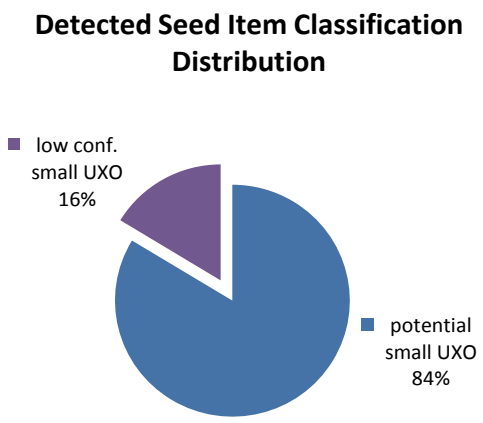

Figure 7. Comparison of target classification distribution between all 983 targets in the seeded area (left) and the 49 detected seeds (right).

8.3.3.2 Detection Results in the Geologically Challenging Western Seed Area

In the western seed area, the Program Office emplaced 110 seeds in a geologically "challenging" environment. These consisted of a mix of 81 mm and 4.2-inch mortars, 105 mm HEAT-rounds (HR), and 105 mm and 155 mm projectiles. Detection results are provided in Table 7. With a detection halo of 0.5 m, 84% of items were detected. Increasing the detection halo resulted in 94% detected at 1.0 m and 96% detected at 1.5 m. At the 1.0 m halo 7 of 12 81 mm mortars, 13 of 14 105 mm HEAT-rounds, all 8 105 mm projectiles and all 52 4.2-inch mortars plus 23 of 24 155 mm projectiles were detected. When the detection halo is increased to 1.5 m, all items except 4 of the 81 mm mortars were detected. Close inspection of the anomalies detected at halos between 1.0 and 1.5 m reveals that the dipole fits were quite poor. The poor fits arise because the default mask is too large and the dipole model is skewed in an effort to fit the underlying geology.

In general, we conduct only a cursory and limited quality control (QC) review of the dipole model fits (rather that the full QC that we would conduct for ground-based surveys where dig/no dig decisions are made). After remasking and reinverting each of these anomalies, the detection results at 1.0 and 1.5 m halo are the same with the exception of one 155 mm projectile. Only part of this anomaly was surveyed at our maximum acceptable ground-clearance of 3.0 m, with any data above that height eliminated from the data used for interpretation. An anomaly was selected by the analyst at a distance of 1.2 m from the seed location, but an acceptable dipole fit could not be obtained. Note that there is one additional 81 mm mortar that was originally placed 1.6 m from the seed location that falls within the 1.0 m detection halo after remasking and inversion.

Table 8 lists the number of seed items assigned to each category compared to the total number of detections in each category. Almost all (99%) of the seed items are placed in the high-probability UXO categories (small, medium, and large), which constitute just over 50% of the total detections.

8.4 TELEMETRY LINK

The DAS recorded data from the moment the helicopter took off until landing. The operator monitored the quality of the collected data and maintained a log that recorded the times when the telemetry link was lost and then regained. This log was used to calculate the percentage of time during survey that the link was maintained. There were three different setup locations used for the telemetry system (refer to Figure 2). The telemetry link was maintained for between 70 and 100% of the time during each survey event. For most survey events, the telemetry link was maintained all the time. Conservatively, we estimate we maintained the link for 95% of the time.

Table 7. Seed detection results in the western seed area.
Results are also shown when several poorly fit anomalies are reinverted.
Statistics on positions were generated using the original inversion results.

Halo Radius	UXO Type	Total # Seeds	# Seeds Detected	Pd	# Seeds Detected Reinverted	Pd Reinverted	Mean (Xi)	Mean (Yi)	Std Dev (Xi)	Std Dev (Yi)	Mean (dist*)	Std Dev (dist)
0.5 m	81 mm	12	6	0.50	7	0.58	0.15	0.07	0.16	0.19	0.26	0.13
0.5 m	105 mm HR	14	11	0.79	12	0.86	0.05	0.06	0.26	0.18	0.30	0.12
0.5 m	105 mm projectile	8	7	0.88	7	0.88	0.12	0.05	0.14	0.07	0.16	0.12
0.5 m	4.2" mortar	52	45	0.87	48	0.92	-0.01	0.08	0.15	0.13	0.18	0.11
0.5 m	155 mm projectile	24	23	0.96	23	0.96	0.01	0.04	0.13	0.14	0.16	0.11
0.5 m	All	110	92	0.84	97	0.88	0.02	0.06	0.17	0.14	0.19	0.12
1.0 m	81 mm	12	7	0.58	9	0.75	0.14	0.14	0.15	0.25	0.30	0.16
1.0 m	105 mm HR	14	13	0.93	14	1.00	0.08	0.11	0.29	0.22	0.34	0.15
1.0 m	105 mm projectile	8	8	1.00	8	1.00	0.08	0.11	0.18	0.19	0.22	0.19
1.0 m	4.2" mortar	52	52	1.00	52	1.00	0.02	0.09	0.27	0.15	0.25	0.20
1.0 m	155 mm projectile	24	23	0.96	23	0.96	0.01	0.04	0.13	0.14	0.16	0.11
1.0 m	All	110	103	0.94	106	0.96	0.04	0.08	0.23	0.16	0.24	0.18
1.5 m	81 mm	12	8	0.67	9	0.75	0.27	0.15	0.39	0.23	0.41	0.35
1.5 m	105 mm HR	14	14	1.00	14	1.00	0.13	0.16	0.34	0.28	0.40	0.26
1.5 m	105 mm projectile	8	8	1.00	8	1.00	0.08	0.11	0.18	0.19	0.22	0.19
1.5 m	4.2" mortar	52	52	1.00	52	1.00	0.02	0.09	0.27	0.15	0.25	0.20
1.5 m	155 mm projectile	24	24	1.00	24	1.00	0.03	0.09	0.17	0.25	0.20	0.24
1.5 m	All	110	106	0.96	107	0.97	0.06	0.10	0.27	0.20	0.27	0.24

*dist = distribution

Table 8. Number of seed items and detected items in each category for the western seed area.

Class Name	Number of Seeds	Number of Detections	% of Seeds	% of Detections
Potential small UXO	12	88	11.2%	3.2%
Potential medium UXO	63	644	58.9%	23.4%
Potential large UXO	31	705	29.0%	25.6%
Total high probability UXO	**106**	**1437**	**99.1%**	**52.2%**
Low confidence small UXO	0	138	0.0%	5.0%
Low confidence medium UXO	0	450	0.0%	16.4%
Low confidence large UXO	0	510	0.0%	18.5%
Low confidence metal	0	54	0.0%	2.0%
Poor dipole fit	1	161	0.9%	5.9%
Total Number	**107**	**2750**		

8.5 NOISE LEVEL

Prior to commencement of the survey, we collected high altitude data to determine the intrinsic system noise levels. We applied the same noise removal methodology to the raw data as was used for the survey data. This methodology involves removing the blade noise using the new de-noising algorithm, applying compensation corrections to the data to remove the effect of changing aircraft attitude, then applying a de-median filter to remove long wavelength signals (e.g. diurnal fluctuations and geologic response) from the data. We calculated the standard deviation of the data in each sensor during one of the high-altitude compensation flights (Table 9). This process overpredicts the noise level as the compensated data do contain some artifacts due to uncorrected heading maneuvers. The intrinsic noise was found to be better than 0.42 nT on all sensors. The noise levels on a 20 sec section of data without large changes in helicopter orientation are reduced by about a factor of two from the noise levels calculated using the entire compensation flight (Table 9). For the vertical gradient, the measured and calculated gradients at the central sensor are approximately the same with a standard deviation of 0.1 nT/m. These standard deviations were computed using the whole calibration flight are larger than the effective intrinsic noise level in the gradient component. On the same 20 sec considered earlier, the standard deviations of both calculated and measured are approximately 0.08 nT/m.

Table 9. Standard deviations of the compensated (but not filtered) high-altitude data.
The average is calculated over all 13 sensors.

Sensor Number	Standard Deviation (nT)	Standard Deviation 20 s Section (nT)	Sensor Number	Standard Deviation (nT)	Standard Deviation 20 s (nT)
1	0.33	0.12	8	0.41	0.30
2	0.37	0.14	9	0.37	0.31
3	0.41	0.15	10	0.34	0.29
4	0.41	0.18	11	0.27	0.26
5	0.39	0.21	12	0.21	0.22
6	0.39	0.24	13	0.20	0.19
7	0.42	0.28			
Average	0.35	0.22			

8.6 ACCURACY OF CALCULATED VERTICAL GRADIENTS

The accuracy of the calculated vertical gradient relative to the measured gradient was established during the test flights at FLBGR. We verified the accuracy using the last validation flight on day 78 (Figure 8). No high-pass filtering (to suppress geology) was applied to either the calculated or measured gradients, but a direct current (DC) correction was applied to the measured gradient so that it best matched the calculated gradient. The measured and calculated gradients agree quite closely, with a correlation coefficient of 0.997. There are some minor differences in gradient measurements around some of the larger anomalies.

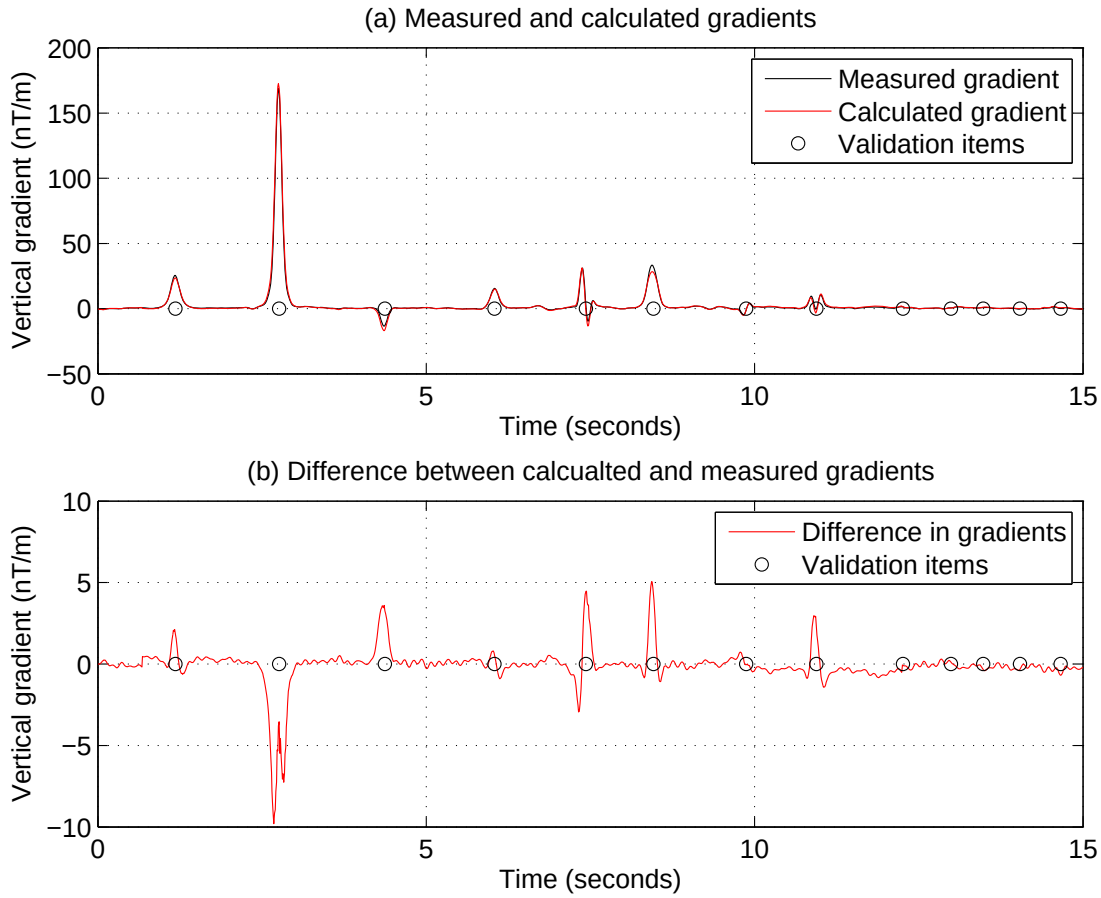

Figure 8. Comparison between measured and calculated gradients over the validation line flown on the last flight of day 78.

8.7 UXO PARAMETER ESTIMATE REPEATIBILITY

Plots of the dipole parameters from the validation lane are shown in Figure 9, with the standard deviations provided in Table 10. The estimated dipole depth was obtained by comparing the elevation predicted by the dipole model with a Light Detection and Ranging (LiDAR) digital elevation model (DEM). There is significant correlated variation day-to-day indicating that there were systematic biases in the GPS elevations.

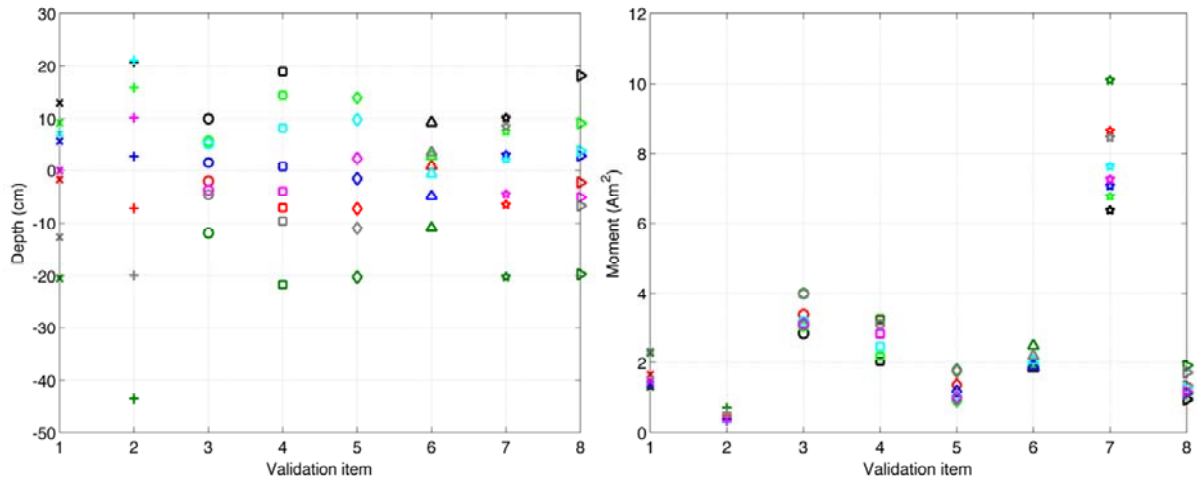

(a) Estimated depth (b) Estimated dipole moment

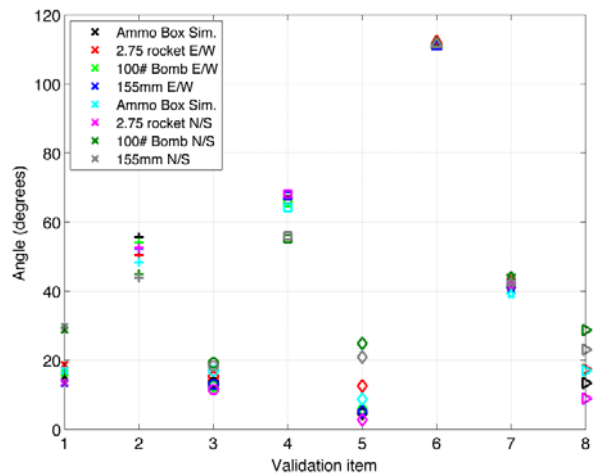

(c) Estimated angle relative to Earth's field

Figure 9. Dipole parameters estimated from the validation lane data.

Table 10. Standard deviations of dipole fit parameters on the validation lane data.

	Easting (cm)	Northing (cm)	Elevation (cm)	Moment (Am^2)	Moment (% of mean)	Angle (degrees)
Ammo box	2.1	7.6	11.5	0.41	24.5	6.5
2.75 rocket E/W	6.1	1.3	22.6	0.13	29.6	4.2
100# bomb E/W	2.2	5.4	7.0	0.43	13.0	2.9
155 mm E/W	6.9	2.4	13.4	0.47	17.1	5.3
Ammo box	1.7	11.0	12.4	0.35	28.4	8.2
2.75 rocket N/S	2.9	0.9	6.5	0.23	11.1	0.5
100# Bomb N/S	3.1	3.1	10.1	1.22	15.7	1.6
155 mm N/S	4.2	7.7	11.3	0.33	24.5	6.7

8.8 OPERATING PARAMETERS

The operating parameters include survey speed, survey altitude, and daily production rates. The daily production rate objective was 300 acres/day. Discounting reflies, downtime for weather and equipment adjustments, the production rate was approximately 290 acres/day (586 acres in 2 survey days). The assessment of the survey altitude and speed was performed by extracting statistics for these parameters from the survey databases. A summary of the survey speed and altitude for each of the sites is shown in Table 11.

Aircraft speed affects the sample density, as well as the survey production rate. The average aircraft speed ranged from 15.8 m/s to 24.6 m/s.

Table 11. Survey altitude and speed for each area.

Area	Speed (m/s)		Altitude (m agl)	
	Mean	Standard Deviation	Mean	Standard Deviation
North-central	21.1	2.9	1.66	0.38
Western seed	18.4	4.0	1.64	0.46
Western	24.6	2.4	1.90	0.42
South-central	24.4	4.0	2.15	0.35
Northeast 1	22.3	5.8	2.00	0.42
Northeast 2	15.8	2.6	2.18	0.38

Survey altitude is the parameter that has the greatest effect on the efficacy of the system for detection of discrete UXO-like ferrous objects. The lowest safe survey altitude achievable at any given time depends on the local site conditions (vegetation, topography, and weather) as well as the skill and comfort level of the pilot. During the demonstration, the pilot was having trouble trying to keep the sensors below 2.0 m agl. Prior experience at this site indicated that it was possible to keep the sensor altitude at an average altitude of 1.5 m agl. After adjustments were made to the boom mount, the survey altitude was reduced to between 1.6 and 1.7 m agl. Unlike the Bell 206L, the MD 530F skid gear is flexible and splays out and up when the aircraft is on the ground. Once weight is removed from the skids, they spring back in and down. Thus, when the aircraft is airborne, the skid gear hangs down about 0.2 m—forcing the pilot to fly higher by this same distance. The previous survey, flown in 2005 with the Bell206L, collected data at 1.5 m agl with very little emphasis placed upon flying as low as possible. On some tests the survey altitude achieved with the Bell206L was as low as 1.0 m.

8.9 ROTOR NOISE SUPPRESSION ALGORITHM

In Figure 10 and Figure 11, we show data from the central sensor that were collected at high-speed over the validation line on day 78. The figures compare raw, low-pass filtered and rotor-suppressed versions of the data. The 6 Hz low-pass and rotor-suppressed data are similar at positions away from the validation lane anomalies with the 6 Hz low-pass data exhibiting significant distortion over the validation lane anomalies. The helicopter is traveling fast and low to the ground, which causes the signal from near-surface anomalies to overlap with that of the rotor-noise. The low-pass filter removes both the rotor-noise and some of the frequency content from the signals of interest (see Figure 11c and d in particular). In contrast, signal integrity is maintained and rotor-noise is eliminated when the rotor-noise suppression algorithm is applied to the data.

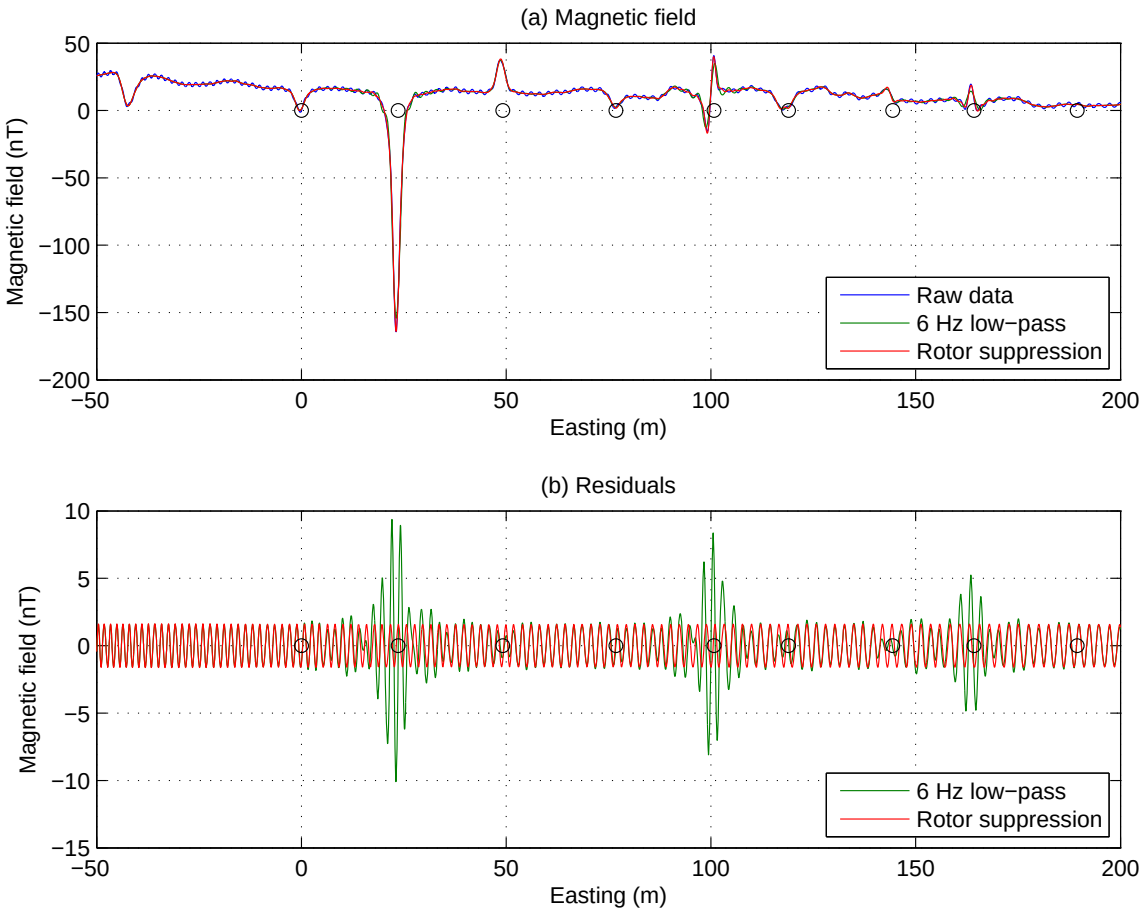

Figure 10. Data from the middle sensor (sensor 7) collected at high-speed over the validation line on day 78.

(a) Compares the raw data with 6 Hz low-pass filtered and rotor suppressed versions of the data. (b) Shows the difference between raw and low-pass filtered data, and between raw and rotor-suppressed data.

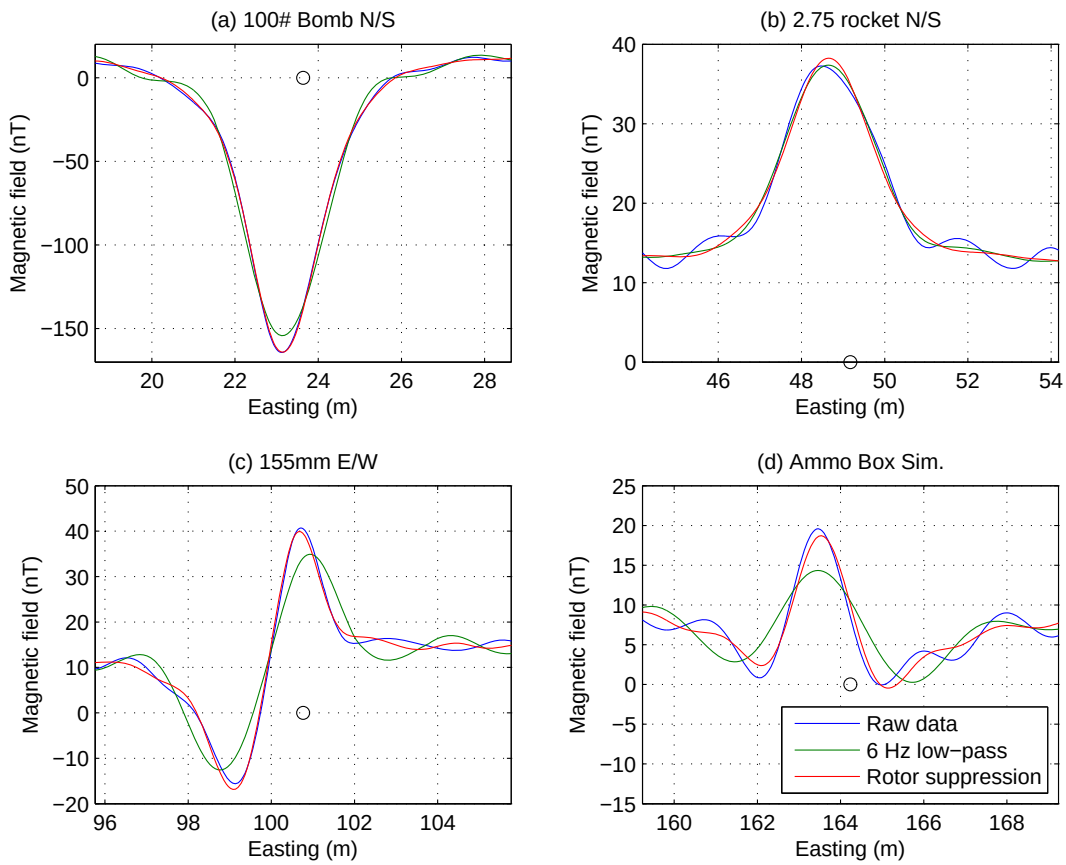

Figure 11. Close-up of validation lane anomalies from Figure 10, showing the difference between the raw data, a 6 Hz low-pass filtered version of the data and the rotor-noise corrected data.

8.10 DATA DENSITY/POINT SPACING

The cross-track data density is essentially static and is a function of the system geometry. With the exception of isolated data gaps (addressed above) the "worst case" spacing is our sensor spacing of 0.75 m. The effective density is much higher than this due to the significant overlap required to minimize data gaps due to the inevitable cross-track variation of the helicopter flight path. However, because the density is not uniform, we quote the "worst case" as the data density achieved. Down-track data density is much higher than the cross-track density and is a function of survey speed. At our final sample rate of 100 Hz, the survey speeds of 15–25 m/s (20–50 kts) resulted in down-line data spacing of 0.15 – 0.25 m.

8.11 SURVEY COVERAGE

As a general practice, images representing the data from each day of survey flying are created to identify areas requiring fill-in flying to cover significant gaps in coverage. Invariably there will be a number of gaps in survey coverage that cannot be practically filled. To estimate the survey coverage performance, at each grid node (5 m intervals) we search through a 1 m radius for a valid data point. We divide the number of grid nodes where valid data are found by the total

number of grid nodes to derive the percentage of survey coverage. Based on these factors and acreages, the final coverage was determined to be 99.2%.

9.0 COST ASSESSMENT

Cost information associated with the demonstration of all airborne technology, as well as associated activities, was tracked and documented before, during, and after the demonstration to provide a basis for determination of the operational costs associated with this technology (Table 12). These costs include both operational and capital costs associated with system design and construction; salary and travel costs for support staff; subcontract costs associated with airborne services, support personnel, and any leased or rented equipment; costs associated with the processing, analysis, comparison, and interpretation of airborne results generated by this demonstration.

Table 12. Cost tracking.

Cost Category	Sub Category	Details	Costs
System modeling and integration	Sensor configuration optimization modeling	Modeling, engineering, testing, and preparation of white papers detailing the results for sensor configuration and telemetry system Installation and initial test flights prior to verify the entire system was operating as designed	$139,150
	Telemetry system design and testing		
	Helicopter noise measurements		
	Boom configuration development and engineering		
Start-up costs	Shakedown test	Includes mobilization to Denver test site, data collection, and analysis of system performance	$228,267
	Demonstration planning	Coordination w/Program Office and KPBR site, preparation of Demonstration Plan	$24,344
Operating costs	Demonstration at KPBR	Data acquisition and associated tasks, including helicopter operation time, mobilization and demobilization from Denver to Albuquerque	$135,532
Data processing and analysis	Data processing, analysis, and reporting	Initial and secondary processing of data, analysis of airborne magnetometry datasets	$37,744
Management	Management and meetings	Project related management, reporting and contracting, IPRs*, presentations, supplemental type certification (STC) evaluation	$99,440
		Total Costs	$664,477
		Total Technology Cost	$197,620
		Acres Surveyed	586
		Unit Cost	$337

*Interim Progress Reviews

The demonstration survey was conducted over 5 days in March 2009. The effort included mobilization and demobilization of the helicopter and project team from Denver to Albuquerque, setup of the validation lane, compensation flights, and data collection over the selected acreage. A total of 586 acres was surveyed. The data collection was effectively completed in 2 days of operation. The remainder of the field effort involved some in-field modifications and adjustments (previously described) and installation and removal of the boom and electronics components from the helicopter. The relatively short distance required to mobilize the helicopter

and equipment for this demonstration helped keep the demonstration costs relatively low. The data collection costs on a per acre basis are similar to those for previous demonstrations of this technology.

The per acre cost to perform the demonstration is inflated relative to expected operational costs for a production survey. The actual data collection was performed over 2 days, while the total duration of the effort was 5 days. The in-field modifications and other test activities took up the remainder of the time in the field. Table 13 presents the projected operational costs for a similar production survey. The per acre cost of $193/acre is consistent with the projected costs for the existing HeliMag technology. Table 14 is taken from the WAA HeliMag Cost and Performance report (Foley and Wright, 2008d), with the estimated cost for a 1000 acre survey at $178/acre. The increased costs for the next generation system reflect the increased number of magnetometers (14 versus seven), costs for the telemetry equipment, and a second DAS (each DAS can accommodate data for seven magnetometers). Costs to deploy the next generation system would decrease with the size and duration of a production survey, similar to the decreasing per acre costs shown in Table 14.

Table 13. Projected costs for 2-day survey using the next generation HeliMag system.

Cost Category	Sub Category	Details	Costs
Start-up costs	Demonstration planning	Coordination w/Program Office and KPBR site, preparation of Demonstration Plan	$24,344
Operating costs	Demonstration at KPBR	Data acquisition and associated tasks, including helicopter operation time, mobilization and demobilization from Denver to Albuquerque	$74,675
Data processing and analysis	Data processing, analysis, and reporting	Initial and secondary processing of data, analysis of airborne magnetometry datasets	$14,348
Total Technology Cost (demonstration preparation, operations, reporting)			$113,367
Acres Surveyed			586
Unit Cost			$193

Table 14. Estimated costs scenarios for helicopter magnetometry.
(Taken from Foley and Wright, 2008d)

Cost Category	1000 Acre Site	5000 Acre Site	7500 Acre Site	10,000 Acre Site
Planning, preparation and management	$32,000	$47,000	$55,000	$62,000
Mobilization/demobilization	$40,000	$40,000	$40,000	$40,000
Data acquisition surveys	$82,000	$410,000	$612,000	$817,000
Data processing, analysis, and GIS products	$12,000	$40,000	$54,000	$67,000
Reporting and documentation	$12,000	$15,000	$20,000	$30,000
Total Costs	**$178,000**	**$552,000**	**$781,000**	**$1,016,000**
Costs per Acre	**$178**	**$110**	**$104**	**$102**

9.1 DATA PROCESSING AND ANALYSIS, REPORTING

Data processing and analysis were conducted between March and July 2009, followed by report preparation. The detailed analyses are described in Sections 6 and 7.

9.2 MANAGEMENT

Management activities have included evaluation of the requirements for obtaining an STC for the modified system on the MD530F helicopter. It was determined, in conjunction with the Program Office, that an STC for this system will be pursued in the future when the system is to be deployed for production surveys. Other management costs included presentations for IPRs and the annual Strategic Environmental Research and Development Program (SERDP)/ESTCP symposia, in addition to general project management activities.

9.3 COST DRIVERS

The major cost driver for an airborne survey system is the cost of aircraft airtime. In terms of tasks, this constitutes a major percentage of the data acquisition costs—the single largest cost item.

9.4 COST BENEFIT

A number of factors should be considered for DoD-wide application of WAA, including data acquisition, when evaluating the appropriateness of helicopter technology and potential for cost savings. Sites must be large enough to justify the deployment of aircraft and equipment to conduct a survey. Climatic conditions and terrain can limit the results of surveys. At amenable sites, the use of helicopter magnetometry can focus the use of ground survey technology and can provide substantial cost savings through footprint reduction.

This page left blank intentionally.

10.0 IMPLEMENTATION ISSUES

As a WAA technology, the Next Generation HeliMag system is subject to the same issues of regulatory acceptance of the methodology as investigated in the WAA Pilot Program. The ESTCP Program Office established a Wide Area Assessment Pilot Program Advisory Group to facilitate interactions with the regulatory community and potential end users of this technology. Members of the Advisory Group include representatives of USEPA, state regulators, USACE officials, and representatives from the Services. The Advisory Group provided valuable feedback on the WAA methodology that is expected to facilitate its acceptance into the wider community. However, there will be a number of issues to be overcome to allow implementation of WAA technologies beyond the pilot program, including decision making regarding areas with no indication of munitions use.

A main challenge of the Pilot Program was to collect sufficient data and perform sufficient evaluation such that the applicability of these technologies to uncontaminated land and their limitations were well understood and documented. Similarly, demonstrating that WAA data can be used to provide information on target areas regarding boundaries, density and types of munitions to be used for prioritization, cost estimation, and planning requires that the error and uncertainties in these parameters are well documented.

Therefore, following successful technology demonstration of the modified HeliMag technology, regulatory acceptance will piggyback on the success of the ESTCP WAA Pilot Program and the overall WAA methodology. This technology will be one more tool in the WAA "toolbox" that provides flexibility for WAA technology selection that can reduce cost of characterization.

This page left blank intentionally.

11.0 REFERENCES

Billings, S. D., and D. Wright. 2009a. ESTCP MM-0741 Next Generation HeliMag UXO Mapping Technology. Final Demonstration Report.

Billings, S. D., and D. Wright. 2009b. Optimal total-field magnetometer configuration for near-surface applications: The Leading Edge, 28, 522-527.

Billings, S. D. 2004. Discrimination and Classification of Buried Unexploded Ordnance Using Magnetometry: IEEE Transactions on Geoscience and Remote Sensing 42, 1241 – 1251.

Foley, J., and D. Wright. 2008a. Demonstration of Helicopter Multi-Sensor Towed Array Detection System (MTADS) Magnetometry at Former Camp Beale, California. ESTCP Final Report, Project MM0535. October.

Foley, J., and D. Wright. 2008b. Demonstration of Airborne Wide Area Assessment Technologies at Kirtland Precision Bombing Range, New Mexico. Final Report. October.

Foley, J., and D. Wright. 2008c. Demonstration of Helicopter Multi-Sensor Towed Array Detection System (MTADS) Magnetometry at Victorville Precision Bombing Range, California. ESTCP Project MM0535 Final Report. December.

Foley, J., and D. Wright. 2008d. Demonstration of Helicopter Multi-Towed Array Detection System (MTADS) Magnetometry Technology for the ESTCP Wide Area Assessment Pilot Program Cost and Performance Report. ESTCP Final Report. October.

Nelson, H.H., J.R. McDonald, D. Wright. 2005. Airborne UXO Surveys Using the MTADS. ESTCP Project 200031 Final Report.

Nelson, H.H, K. Kaye, and A. Andrews. 2008. ESTCP Pilot Project Wide Area Assessment for Munitions Response, Final Report. Environmental Security Technology Certification Program Office (DoD) Final Report. July.

Siegel, R. M. 2008. Simultaneous Magnetometer and EM61 MK2 Vehicle-Towed Array for Wide Area Assessment Draft Final Report.

Tuley, M., and E. Dieguez. 2005. Analysis of Airborne Magnetometer Data from Tests at Isleta Pueblo, New Mexico, February 2003. Technical Report, MM-0037. May.

Versar. 2005. Former Kirtland Precision Bombing Range, Conceptual Site Model, V3. Prepared for ESTCP Program Office.

Wright, D.J., J.R. McDonald, N. Khadr, and H.H. Nelson. 2002. Dynamic sensor positioning in three dimensions on an airborne platform. Published in Proceedings UXO/Countermine Forum.

This page left blank intentionally.

APPENDIX A

POINTS OF CONTACT

Point of Contact	Organization	Phone Fax E-Mail	Role
Dr. Stephen Billings	Sky Research, Inc. Suite 112A 2386 East Mall Vancouver, BC, V6T 1Z3 Canada	Phone: 541-552-5185 E-mail: Stephen.Billings@skyresearch.com	Co-Principal Investigator
David Wright	Wright Research and Design 9500 Kingsford Drive Cary, NC 27511	Phone: 919-520-8673 E-mail: david.wright@wrandd.com	Co-Principal Investigator
Ms. Joy Rogalla	Sky Research, Inc. 445 Dead Indian Road Ashland, OR 97520	Phone: 541-552-5104 Fax: 541-488-4606 E-mail: Joy.Rogalla@skyresearch.com	Project Manager
Dr. Herbert Nelson	ESTCP Program Office 901 North Stuart Street Suite 303 Arlington, VA 32203	Phone: 703-696-8726 Fax: 703-696-2114 E-mail: Herbert.Nelson@osd.mil	Contracting Officer's Technical Representative

ESTCP Program Office

901 North Stuart Street
Suite 303
Arlington, Virginia 22203

(703) 696-2117 (Phone)
(703) 696-2114 (Fax)

E-mail: estcp@estcp.org
www.estcp.org